NeuroImage 64 (2013) 341–355

Contents lists available at SciVerse ScienceDirect

NeuroImage

journal homepage: www.elsevier.com/locate/ynimg

Pharmacological modulation of brain activity in a preclinical model of osteoarthritis

Jaymin Upadhyay [a,*,1], Scott J. Baker [a,1], Rajasimhan Rajagovindan [a,1], Michelle Hart [b,1], Prasant Chandran [a], Bradley A. Hooker [a], Steven Cassar [a], Joseph P. Mikusa [c], Ann Tovcimak [a], Michael J. Wald [a], Shailen K. Joshi [c], Anthony Bannon [c], Jeroen K. Medema [d], John Beaver [a], Prisca Honore [b], Rajesh V. Kamath [b], Gerard B. Fox [a], Mark Day [a]

[a] Translational Sciences, Advanced Technology, Global Pharmaceutical Research and Development, Abbott Laboratories, Abbott Park, IL, USA
[b] Immunology Discovery, Abbott Bioresearch Center, Global Pharmaceutical Research and Development, Abbott Laboratories, Worcester, MA, USA
[c] Neuroscience Discovery, Global Pharmaceutical Research and Development, Abbott Laboratories, Abbott Park, IL, USA
[d] Immunology Development, Global Pharmaceutical Research and Development, Abbott Laboratories, Abbott Park, IL, USA

ARTICLE INFO

Article history:
Accepted 30 August 2012
Available online 7 September 2012

Keywords:
Osteoarthritis
Pain
phMRI
Functional connectivity
Matrix metalloproteinase inhibition
Celecoxib

ABSTRACT

The earliest stages of osteoarthritis are characterized by peripheral pathology; however, during disease progression chronic pain emerges—a major symptom of osteoarthritis linked to neuroplasticity. Recent clinical imaging studies involving chronic pain patients, including osteoarthritis patients, have demonstrated that functional properties of the brain are altered, and these functional changes are correlated with subjective behavioral pain measures. Currently, preclinical osteoarthritis studies have not assessed if functional properties of supraspinal pain circuitry are altered, and if these functional properties can be modulated by pharmacological therapy either by direct or indirect action on brain systems. In the current study, functional connectivity was first assessed in order to characterize the functional neuroplasticity occurring in the rodent medial meniscus tear (MMT) model of osteoarthritis—a surgical model of osteoarthritis possessing peripheral joint trauma and a hypersensitive pain state. In addition to knee joint trauma at week 3 post-MMT surgery, we observed that supraspinal networks have increased functional connectivity relative to sham animals. Importantly, we observed that early and sustained treatment with a novel, peripherally acting broad-spectrum matrix metalloproteinase (MMP) inhibitor (MMPi) significantly attenuates knee joint trauma (cartilage degradation) as well as supraspinal functional connectivity increases in MMT animals. At week 5 post-MMT surgery, the acute pharmacodynamic effects of celecoxib (selective cyclooxygenase-2 inhibitor) on brain function were evaluated using pharmacological magnetic resonance imaging (phMRI) and functional connectivity analysis. Celecoxib was chosen as a comparator, given its clinical efficacy for alleviating pain in osteoarthritis patients and its peripheral and central pharmacological action. Relative to the vehicle condition, acute celecoxib treatment in MMT animals yielded decreased phMRI infusion responses and decreased functional connectivity, the latter observation being similar to what was detected following chronic MMPi treatment. These findings demonstrate that an assessment of brain function may provide an objective means by which to further evaluate the pathology of an osteoarthritis state as well as measure the pharmacodynamic effects of therapies with peripheral or peripheral and central pharmacological action.

Introduction

Pain amelioration is a major goal of therapeutic approaches to osteoarthritis. Clinical trials of novel treatments commonly utilize endpoints such as subjective pain ratings or the Western Ontario and McMaster Universities Osteoarthritis Index (WOMAC) to determine if an analgesic effect is achieved. These patient-reported behavioral endpoints are essential for clinical development, but differ greatly from the types of pain indices that can be assessed in early, preclinical phases of new drug evaluation. Since the latter are primarily reflexive in nature and do not probe affective components of pain, they may be of limited translational value for understanding chronic pain states in humans. Here we employed neuroimaging to investigate whether a preclinical model of osteoarthritis is associated with functional changes in supraspinal pain circuitry, and whether such functional plasticity can be impacted by a disease-modifying osteoarthritis drug or compounds with analgesic capabilities.

In osteoarthritis, peripheral trauma initially occurs within one or more joints (Heinegard and Saxne, 2011). Dynamic biological processes (articular cartilage degradation, osteophyte formation and synovial inflammation) present at the periphery are thought to be the root cause of initial joint pain and loss of joint mobility, both of

* Corresponding author. Fax: +1 847 938 5286.
E-mail address: jaymin.upadhyay@abbott.com (J. Upadhyay).
[1] These authors contributed equally to this manuscript.

1053-8119/$ – see front matter © 2012 Elsevier Inc. All rights reserved.
http://dx.doi.org/10.1016/j.neuroimage.2012.08.084

which can lead to changes in quality of life. Although the correlation between joint trauma and pain experienced by patients has not yet been fully established, it is well known that long-term manifestations of pain and behavioral changes are associated with plasticity in the brain (Gwilym et al., 2010; Woolf and Salter, 2000). A further understanding of this neuroplasticity, specifically that which occurs in supraspinal pain circuitry, may enable a more complete characterization and comparison of the pathogenesis of preclinical models of osteoarthritis and that of osteoarthritis patients. One means through which plasticity in the brain in an osteoarthritic state can be evaluated is by measuring functional connectivity within supraspinal pain circuitry, where the degree of functional connectivity within this circuitry in chronic pain patients has been previously observed to correlate with subjective measures of pain (Baliki et al., 2010; Napadow et al., 2010).

In the *Part I* of this study, we characterized the supraspinal resting-state functional connectivity in the rodent medial meniscus tear (MMT) model of osteoarthritis, a surgical model designed to possess knee joint trauma (articular cartilage degradation) and a pain state (mechanical hypersensitivity) lasting for 5–6 weeks post-surgical procedures. This initial assessment of the MMT model occurred at 3 weeks post-surgery. Given that MMT animals are known to have a sustained pain state over several weeks, alterations in brain function as measured by functional connectivity may be present. Although the induction of pain is of course distinct between MMT animals and osteoarthritis or other pain patient populations, similarities with respect to directionality of functional connectivity changes may exist between preclinical and clinical populations. To probe functional connectivity changes in the MMT model, the nucleus accumbens (NAcc) as well as the ventral posterior lateral thalamus (VPL) were used as seed regions. While the NAcc, a medial pain pathway structure, has been shown to mediate motivational and reward-aversion aspects of pain processing (Baliki et al., 2010; Becerra et al., 2001), the VPL, a lateral pain pathway structure, has long been known to facilitate sensory (e.g., intensity or localization) components of pain (Chung et al., 1986; Kenshalo et al., 1980). To determine if pharmacological treatment can attenuate neuroplasticity within pain mediating circuitry present in MMT animals at 3 weeks post-surgery, we also measured the effects of a novel, broad-spectrum matrix metalloproteinases inhibitor (MMPi), which has a peripheral mechanism of action. MMPs are a family (28 members) of endogenous, extracellular enzymes that are implicated in a variety of pathological processes such as tumor progression (Fang et al., 2000) and central nervous system diseases states (Yong et al., 2001). With respect to osteoarthritis, MMPs such as MMP-2, MMP-9 and MMP-13 are expressed and functional during tissue or cartilage degradation, and play a role in cleaving collagen (i.e., type I, type II and type IX collagen) as well as fibromodulin (Heathfield et al., 2004; Itoh et al., 2002). Recently, MMP-2 and MMP-9 activity have been implicated in the induction and maintenance of neuropathic pain, respectively (Kawasaki et al., 2008). In the current investigation, we hypothesized that if peripheral trauma (i.e., articular cartilage degradation) could be reduced by MMPi beginning at a very early stage, central changes (i.e., functional neuroplasticity), if present, would likewise be reduced, specifically within supraspinal pain mediating circuitry. Furthermore, the study of MMPi from a functional connectivity perspective is of particular importance given that it has yet to be demonstrated if a disease-modifying osteoarthritis treatment that mitigates predominately peripheral events can hinder supraspinal neuroplasticity from occurring, the latter of which may be pathologic in nature.

In *Part II* of this investigation, the pharmacodynamic effects of celecoxib (Celebrex, Pfizer, Inc.), a selective cyclooxygenase-2 (COX-2) inhibitor, were evaluated in MMT and sham animals at 5 weeks post-surgery. Celecoxib, along with other non-steroidal anti-inflammatory drugs, is a common therapeutic choice to treat pain in osteoarthritis patients. Inhibition of COX-2 subsequently hinders synthesis of prostaglandin E_2 (PGE_2), which plays a key role in both peripheral and central sensitization to pain (Samad et al., 2001; Vanegas and Schaible, 2001). Work by Ciceri et al. quantified the central drug action of celecoxib in brain structures such as the hippocampus, and demonstrated the down-regulation of PGE_2 in the brain (Ciceri et al., 2002). This study suggests that the central pharmacology of celecoxib is considered to substantially contribute to its analgesic efficacy (Cashman, 1996; Ciceri et al., 2002). To date, the in vivo body of work where celecoxib has been evaluated in the context of pain and analgesia has primarily focused on preclinical behavioral readouts assessing thermal and mechanical hypersensitivity (Ferland et al., 2011). The extent to which celecoxib functionally modulates supraspinal circuitry has not been previously characterized using in vivo methods such as phMRI. Thus, we aimed to measure the phMRI[2] infusion responses as well as modulation of functional connectivity elicited by acute intravenous (IV) administration of celecoxib in MMT and sham cohorts in order to further define the mechanism of action (MOA) of celecoxib at a systems level. We hypothesized that given the known peripheral and central drug action of celecoxib as well as its pharmacokinetic PK properties (Paulson et al., 2000), pharmacodynamic effects on pain circuitry function by celecoxib could be measured with phMRI and functional connectivity and compared with the peripheral pharmacological action of MMPi. For functional connectivity analysis, seed region selection could be guided by the observed phMRI response. Furthermore, based on previous descriptions of COX-2 expression in the rat brain (Breder et al., 1995; Yamagata et al., 1993), celecoxib was hypothesized to regulate pain circuitry structures such as the hippocampus and amygdala. However, it was considered that phMRI and functional connectivity methodology would enable a determination of a broad range of brainstem, subcortical and cortical structures possibly affected by selective COX-2 inhibition in MMT animals.

Materials and methods

Animals

All studies were conducted at Abbott Laboratories in accordance with Institutional Animal Care and Use Committee (IACUC) guidelines and the National Institutes of Health Guide for Care and Use of Laboratory Animals. Abbott Laboratories facilities are accredited by the Association for the Assessment and Accreditation of Laboratory Animal Care (AAALAC).

MMT and sham surgical procedures

The unilateral sham and MMT model surgical procedure has been previously characterized (Bove et al., 2006). During the MMT surgical procedure (animals' right knee), an arthrotomy was performed to expose the joint and the medial collateral ligament was transected to expose the medial meniscus. The medial meniscus was subsequently excised at its narrowest point. The exposed joint was then closed and the skin was approximated (sutured or glued). In the sham surgeries (animals' right knee), arthrotomies were performed where the joint was exposed and the medial collateral ligament was transected to expose the medial meniscus. The incision site was then closed. This sham surgical procedure controls for any effects resulting from the medial collateral ligament transection. The sham procedure by itself does not yield long-term joint destruction or behavioral changes as measured by hindpaw weight distribution (Bove et al., 2006). The exploratory incision in MMT sham surgery can induce mechanical pain for several days while the wound heals (data not shown); however, this specific pain subsides to near baseline levels by the end of week 1, well prior to when the animals were tested. At weeks 3–5, MMT

[2] In the current study, phMRI is referred to as a technique enabling the infusion response to a pharmacological compound to be measured.

animals show significantly ($p<0.01$; two-tailed, t-test; $n=8$–10/cohort) greater mechanical hypersensitivity relative to sham and naïve animals, while sham and naïve animals show no indications of mechanical hypersensitivity during this time interval (historical, in-house data). Mechanical hypersensitivity was assessed with Semmes–Weinstein monofilaments (Stoelting Co., Wood Dale, IL) using the Dixon up-down method (Chaplan et al., 1994). Specifically, mechanical hypersensitivities were measured using von Frey filaments of varying force. Two trials per time point on the paw were analyzed using the Dixon up-down method and averaged to give the stimulus at which there was a 50% probability of a withdrawal. Filaments were applied in and around the center (+/−10 mm) of the hind paw plantar surface.

Part I: MMT and MMPi treatment effect

Properties of MMPi

MMPi (biaryl ether retro-hydroxamate) is a broad-spectrum, matrix metalloproteinase (MMP) inhibitor. MMPi has potency for MMP-2 ($IC_{50}=0.78$ nM), MMP-8 ($IC_{50}=5.00$ nM), MMP-9 ($IC_{50}=0.50$ nM) and MMP-13 ($IC_{50}=0.30$ nM) (Gum et al., 2001). The potency is less for other MMPs; MMP-1 ($IC_{50}=8900$ nM), MMP-3 ($IC_{50}=12.00$ nM) and MMP-7 ($IC_{50}=11{,}000$ nM). Following acute oral dosing of 30 mg/kg MMPi in rat, plasma $t_{1/2}$ and C_{max} were measured to be 6.6 h and 8.96 μg/ml, respectively. At 3 weeks following 30 mg/kg MMPi PO BID dosing in 6 adult male Lewis rats, MMPi levels measured in plasma, brain and spinal cord were 7.9 ± 0.8 μg/ml (~16 nM), 0.6 ± 0.1 μg/g (~1 nm/g) and 0.5 ± 0.1 μg/g (~1 nm/g). Brain and spinal cord-to-plasma ratios following 30 mg/kg MMPi PO BID dosing for 3 weeks were 0.08 and 0.06 respectively. Plasma, brain and spinal cord samples were obtained between 6 and 7 h after the first daily dose of MMPi. Brain and spinal cord vasculature was not perfused prior to extraction or measurement of MMPi levels. Lastly, MMPi was found to have an efflux ratio of 21.2 in the MDCK-MDR1 assay, suggesting that MMPi is a P-glycoprotein (P-gp) substrate and thus is considered to have poor brain penetrance and exposure. Typically, an efflux ratio >2 indicates a P-gp substrate.

Functional MRI study

Adult male Lewis rats (Charles River, Portage, MI) were used in this study ($n=22$; 225–250 g at start of study). The current study contained 2 sham cohorts and 2 MMT model cohorts (Fig. 1A):

(i.) Sham (vehicle (VEH)) ($n=5$)
(ii.) MMT (VEH) ($n=6$)
(iii.) Sham (MMPi) ($n=5$)
(iv.) MMT (MMPi) ($n=6$)

The VEH condition consisted of 0.02% Tween 80/2% HPMC PO BID dosing, while the MMPi condition consisted of 30 mg/kg MMPi PO BID dosing. VEH or MMPi dosing began on the same day as the sham or MMT surgery and continued throughout the course of the study. MMT and sham surgeries were performed in a randomized and staggered manner over the course of a 1-week period, while each subject underwent resting-state functional connectivity scanning prior to surgical procedures (week 0) and also, post-surgery (week 3). Animals were scanned in the same order as the MMT or sham surgeries. Animals were group-housed (2 per cage) in temperature-controlled (22–24 °C) rooms and maintained on a 12:12 light:dark cycle with lights on at 6:00 am. Rat chow and water were provided ad libitum.

Resting-state fMRI acquisition

All MRI scanning was performed on a 4.7 T Bruker Pharmascan (Karlsruhe, Germany) MRI magnet, with a 72 mm diameter transmit volume coil and a quadrature surface receiver coil. For MRI data collection, animals were placed under light isoflurane (2%) anesthesia using room air as a carrier gas. A small bite loop was used to position and hold the head in a nose cone used for delivery of the gas; no other restraint was necessary. Animals were placed in a prone position on a movable MRI-compatible bed, which was heated by an embedded circulating water bath to maintain a physiologically normal body temperature, negating any anesthetic effect on thermal auto-regulation. Animals were imaged between 4 and 7 h after the first daily dose of VEH or MMPi. High-resolution anatomical MRI data were collected using a T2-weighed RARE sequence. Anatomical MRI parameters: echo time = 75 ms, time of repetition = 3300 milliseconds, spatial

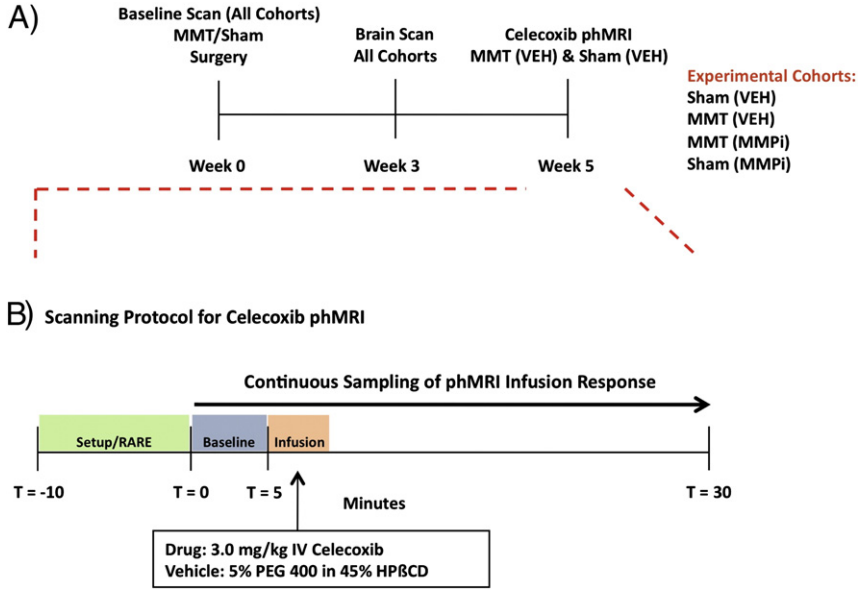

Fig 1. Study protocol. (A) Across a 5-week time period, 3 scanning sessions took place. At week 0, all MMT and sham animals were scanned prior to surgical procedures in order to obtain a baseline measurement. At week 3, an assessment of the effects of the MMT surgical procedure relative to sham, as well as an assessment of the chronic MMPi treatment effect was performed. (b) At week 5, only the MMT (VEH) and Sham (VEH) cohorts underwent the phMRI protocol, where the acute pharmacodynamic effects of celecoxib were evaluated. Here, animals were included in a randomized, vehicle controlled, crossover phMRI study. For the phMRI scan, 5 min of baseline was collected prior to intravenous administration of vehicle or 3.0 mg/kg IV celecoxib. The red dashed lines indicate that the depicted phMRI scanning protocol was performed only at week 5. The same study protocol was implemented for Study 1 (MMT + sham) and Study 2 (MMT only) (see also Fig. 7).

resolution = 0.25 × 0.25 × 1.25 mm and number of slices = 14 coronal slices. To measure resting-state functional connectivity, a single-shot gradient echo planar imaging pulse sequence was utilized with parameters that enabled the measurement of blood oxygenated level-dependent (BOLD) signal. Resting-state fMRI parameters: echo time = 11.11 ms, time of repetition = 2000 ms, repetitions = 150 (5 min), spatial resolution = 0.5 × 0.5 × 1.25 mm and number of slices = 14 coronal slices.

Resting-state, functional connectivity analysis

Resting-state, functional connectivity data analysis was performed using FMRIB Software Library (FSL 4.1) (www.fmrib.ox.ac.uk/fsl) and VivoQuant 1.20 (Invicro LLC, Boston, MA). The initial preprocessing procedures and single-subject general linear model (GLM) based, seed region functional connectivity analysis of fMRI data was carried out with FSL's FMRI Expert Analysis Tool (FEAT) with local autocorrelation correction. Initially, the first 4 volumes from each resting-state dataset were discarded. The following processing steps were performed to the remaining 146 volumes: (1) motion correction with FMRIB's Linear Motion Correction tool (MCFLIRT), (2) segmentation of the brain from the skull and surrounding tissue for fMRI and RARE (anatomical) images using VivoQuant 1.20 (Invicro LLC, Boston, MA), (3) spatial smoothing with a 1 mm FWHM Gaussian spatial filter, (4) band-pass filtered between 0.01 and 0.1 Hz, thus removing the linear drift artifact and high frequency noise, and (5) co-registration to an in-house rat atlas template (Paxinos and Watson, 2009). Warping of individual datasets to the rat atlas was performed with FMRIB's Linear Image Registration Tool (FLIRT) with a 12 degree-of-freedom affine transformation. During the co-registration procedure, a lower resolution T2-weighted RARE anatomical image was used as an intermediary volume between the resting-state fMRI dataset and an in-house, high-resolution rat anatomical template.

Four distinct functional connectivity analyses were performed where either the left (L, contralateral to surgical knee) nucleus accumbens (NAcc), right (R, ipsilateral to surgical knee) NAcc, left ventral posterior lateral thalamus (VPL) or right VPL was used as a seed regions. In the rodent brain, the NAcc, which is bounded entirely by the ventral striatum, consists of a core and shell region. Given the implemented resolution of the fMRI scan procedure used in the present study as well as the relatively small size of the rat brain, we were not able to differentiate precisely between the NAcc core and shell. Thus, by default, both aspects of the NAcc were incorporated in the NAcc seed region. Likewise, functional connectivity and phMRI changes occurring specifically within the NAcc core or shell could not be ascertained. Such issues stemming from fMRI spatial resolution were not problematic when functionally evaluating the rodent caudate–putamen (bounded entirely by the dorsal striatum) since this is a large subcortical structure that is accurately resolved in the fMRI data (see below for caudate–putamen based seed region analysis). In the functional connectivity analysis, either the NAcc_L, NAcc_R, VPL_L or VPL_R left or right hemisphere time course was used as the main explanatory variable (EV), and subject-specific white matter and cerebral spinal fluid (CSF) time courses were used as confound EVs. White matter and CSF regions were manually identified for each subject prior to any spatial smoothing. The subject level (first level) analysis was performed on both week 0 and week 3 datasets and the parameter estimates from week 0 (baseline) were employed as voxelwise covariates for subsequent group-level comparisons of week 3 parameter estimates to control for any baseline differences between the groups. A subsequent comparison of functional connectivity results at week 3, with and without baseline correction, yielded insignificant differences between the two types of functional connectivity analyses (data not shown). For this study, the addition of voxelwise parameter estimates obtained from the baseline measurements, and used as voxelwise covariates yielded little benefit or difference in determining effect of the MMT surgery or MMPi treatment. Furthermore, by incorporating the baseline correction, unwanted variability was not introduced in the analyses that may have stemmed from factor such as initial exposure from an anesthetic.

Group-level comparisons of interest included (i) MMT (VEH) vs. Sham (VEH) to characterize the MMT-induced changes in supraspinal pain circuitry, (ii) MMT (VEH) vs. MMT (MMPi) to test if MMPi reversed MMT-induced changes in brain functional connectivity and (iii) Sham (VEH) vs. Sham (MMPi) to characterize MMPi induced central nervous system (CNS) effects in sham animals. FSL's mixed-effects FLAME 1 analysis was employed to perform between-group comparisons (Jbabdi et al., 2009). Single-subject contrast of parameter estimate maps were then projected onto a standard template for visualization. Here, parameter estimates defined the statistical similarity between the main EV (i.e., NAcc_L time course) and voxelwise time course profile. Moreover, given that contrast of parameter estimate maps for each subject were co-registered to the standard template, parameter estimates averaged over the region of interest (i.e., overlap region or atlas defined region) could be extracted for each subject. The mean was then taken for each cohort and for each region. Each group-level z-statistic map resulting from the mixed-effects analysis was thresholded using clusters determined by $Z > 1.6$ and a (corrected) cluster significance threshold of $p = 0.05$. An analysis of variance (ANOVA) analysis ($\alpha = 0.05$) of parameter estimates for each of the four seed region analyses (NAcc_L, NAcc_R, VPL_L and VPL_R) was also performed to identify overall inter-cohort differences.

Cartilage degradation study

Adult male Lewis rats (Charles River, Portage, MI) were used in this study ($n = 46$; ~280–300 g at start of the study). This study included:

(i.) Sham ($n = 6$)
(ii.) MMT (VEH) ($n = 20$)
(iii.) MMT (MMPi) ($n = 20$)

The VEH condition consisted of 0.02% Tween 80/2% hydroxypropylmethylcellulose (HPMC) PO BID dosing, while the MMPi condition consisted of 30 mg/kg MMPi PO BID dosing. VEH or MMPi dosing began the night before the sham or MMT surgery and continued throughout the course of the study. Animals were group-housed (3 per cage) in temperature-controlled (22–24 °C) rooms and maintained on a 12:12 light:dark cycle with lights on at 6:00 am. Rat chow and water were provided ad libitum. The effects of the MMT surgery and MMPi treatment on articular knee cartilage of male Lewis rats were assessed using histology (toluidine-blue staining) 3 weeks post-surgery.

Part II: MMT and celecoxib treatment effect

At week 5 post-surgery, animals from the MMT (VEH) and Sham (VEH) treatment conditions were utilized in order to characterize the effects of celecoxib in a vehicle controlled, crossover study paradigm (Fig. 1A). One animal in the Sham (VEH) cohort died between weeks 4 and 5. The second part of this investigation also enabled a further utilization of the current set of animals. Moreover, over the course of the investigation, an additional 6 MMT rats (also 5 weeks post-surgery) were available. This latter cohort received no pharmacological or vehicle treatment throughout their lifetime. Therefore, these MMT animals ($n = 6$) were incorporated in this imaging study (vehicle controlled, crossover study paradigm) to assess the consistency of the pharmacodynamic effects of celecoxib as measured by phMRI methodology across experiments.

IV administration of 3.0 mg/kg celecoxib and vehicle

The effects of 3.0 mg/kg IV celecoxib relative to vehicle (5% PEG 400 in 45% HPßCD) were investigated in the phMRI portion of the

investigation. Celecoxib was purchased from Toronto Research Chemicals, Toronto, Canada. We chose a calculated IV dose of celecoxib (3.0 mg/kg) that would reproduce plasma exposure levels as the acute intraparenteral ED_{50} dose (30 mg/kg) observed during evaluation of mechanical hypersensitivity behavioral measures. Effects of celecoxib were evaluated using the Dixon up-down method for von Frey stimulation (Chaplan et al., 1994). Previous pharmacokinetic work in male rats has demonstrated that at a 1 mg/kg IV celecoxib dose, $t_{1/2}$ and clearance is ~3.73 h, 7.76 ml/min/kg, respectively (Paulson et al., 2000). T_{max} in plasma occurs in close proximity of IV administration of celecoxib and well within the 30-min time frame of the phMRI scan. During the phMRI scan, a 5-min baseline was collected prior to the infusion of celecoxib + vehicle or vehicle (Fig. 1b). Celecoxib was intravenously administered via tail vein and over the course of a ~2-min period. The total volume and rate of infusion were 0.8 mL and 24 mL/h, respectively.

PhMRI data acquisition and analysis

All phMRI data was collected on the same 4.7 T Bruker system and under the same experimental conditions as that described for *Part I* of the study. However, the number of repetitions utilized in the phMRI scan was increased to 900 in order to span the 30-min time period. All other anatomical MRI and fMRI data acquisition parameters were constant between *Part I* and *Part II*.

Preprocessing of phMRI data was also same as that described above in 'Resting-state, functional connectivity analysis.' However, Following preprocessing procedures, single-subject, general linear model (GLM) analysis of phMRI data enabled a determination of which brain structures had an increase or decrease in BOLD activity subsequent to 3.0 mg/kg IV celecoxib. The univariate phMRI data analysis was performed using FSL's FMRI Expert Analysis Tool (FEAT) with local autocorrelation correction (www.fmrib.ox.ac.uk/fsl). The design matrix incorporated in the GLM analysis comprised the following explanatory variables (EVs): The main EV, modeling the effects administration of 3.0 mg/kg IV celecoxib or vehicle administration, consisted of a ramp function that followed the infusion paradigm for each drug. The ramp period was set to 2 min. The time during the scan at which the phMRI signal increased or decreased from baseline, or the time at which the plateau phase was reached in response to 3.0 mg/kg IV celecoxib could slightly vary depending on CNS structure or the subject. To enable a more accurate modeling of the phMRI infusion response and capture potential temporal variability, 3 additional regressors were created using VivoQuant (Invicro LLC, Boston, MA) and included as covariates in the GLM analysis (Pendse et al., 2010). Furthermore, a linear drift term, along with subject-specific white matter and CSF time courses, was included in the design matrix as confound EVs. The same GLM model was utilized to analyze all 3.0 mg/kg IV celecoxib and respective vehicle datasets from sham and MMT animals.

GLM-based, seed region functional connectivity analysis was also performed using the phMRI datasets. For functional connectivity analysis, the preprocessed single-subject phMRI datasets were initially band-pass filtered between 0.01 and 0.1 Hz, thus removing the linear drift artifact and high frequency noise. Subsequent to band-pass filtering, subject-specific time courses from the left and right caudate–putamen (CaPu: Seed Region), white matter and cerebral spinal fluid were extracted. The CaPu was chosen as a seed region based on the robust phMRI signal measured in this structure (see Results) as well as the key role the CaPu plays in multiple aspects of pain processing (Borsook et al., 2010; Upadhyay et al., 2011a). Furthermore, based on the unilateral nature of the MMT and sham surgical procedure, distinct left and right hemisphere CaPu based functional connectivity analyses were performed, to identify any hemisphere specific functional connectivity alterations. In the seed region, functional connectivity analysis, either the left or right hemisphere CaPu time course was used as the main EV, while subject-specific time courses from the white matter and CSF were used as confound EVs. While the right hemisphere is ipsilateral to the MMT or sham surgical knee, the left hemisphere is contralateral.

To measure the effects of celecoxib on functional connectivity, the last 5 min of the 30-min phMRI scan was assessed. Functional connectivity was specifically evaluated at the last 5 min, based on the fact that during this time interval, drug exposure was at the greatest extent and a stable phMRI signal was achieved. Functional connectivity was also measured for the first 5 min or pre-infusion period (Fig. 1b). This 5-min pre-infusion period was used to further characterize the underlying differences in functional connectivity between the MMT and sham cohort.

All group-level analysis for phMRI and CaPu based functional connectivity analysis was performed using FSL's mixed-effects FLAME 1 method (Woolrich et al., 2009). This is similar to that which is described above in *Part I*. Each group-level statistical map resulting from the mixed-effects analysis was thresholded at $p<0.05$ and cluster-size thresholded at $p=0.05$.

Results

Effects of the MMT surgery and MMPi treatment on functional connectivity

At 3 weeks post-MMT or sham surgery, the MMT (VEH) cohort demonstrated significantly greater functional connectivity in comparison to the Sham (VEH) cohort (Figs. 2 and 3). This hyper-functional connectivity was observed in NAcc (Figs. 2A and 3A) and VPL (Figs. 2B and 3B) based functional connectivity analyses, and was significantly decreased by MMPi treatment (MMT (MMPi) cohort). The effect of the MMT surgery and MMPi treatment on NAcc functional connectivity was primarily observed within brainstem and other subcortical regions, whereas the surgical and treatment effect on VPL functional connectivity was expanded to cortical regions as well. For example, in comparing NAcc and VPL based functional connectivity results, modulation of functional connectivity within the insula was primarily observed when the VPL_R was used as a seed region (Fig. 2B). Although both the VPL and insula are well implicated in pain and somatic sensation, direct efferent and afferent projections between the two structures are unknown (Craig et al., 2000; Ostrowsky et al., 2002). Thus, the functional connectivity between the VPL and insula as well as any modulatory effects elicited from the MMT procedure or MMPi treatment condition is driven by indirect connectivity between two structures.

The inhibitory effect of MMPi on functional connectivity changes can be observed within the mixed-effects, group-level statistical comparisons (MMT (MMPi) vs. MMT (VEH)) and the line graph shown in Figs. 2C and 3C. For Figs. 2C and 3C, parameter estimates were extracted from example brain regions where functional connectivity of MMT (VEH) > Sham (VEH) and MMT (MMPi) < MMT (VEH) was detected (i.e., bed nucleus of the stria terminalis (BNST) for NAcc_R-based functional connectivity analysis and periaqueductal gray (PAG) for VPL_R-based functional connectivity analysis). The BNST is a component of the cortical–striatal–pallidal system and involved in the affective aspect of pain (Deyama et al., 2007; Morano et al., 2008). On the other hand, the PAG is a key neural substrate of the ascending (spinothalamic) and descending pain systems (Linnman et al., 2011). The ANOVA analysis of parameter estimates obtained from functional connectivity analysis revealed significant inter-group differences for the various functional interactions depicted in Figs. 2 and 3 (Table 1). Here, parameter estimates were extracted from the entire atlas defined regions of interest as oppose to a specific region of overlap. In Fig. 3C, the trends in functional connectivity across the 4 cohorts are given for the NAcc_L-ventral tegmental area (VTA). The VTA was chosen given its direct connectivity with the NAcc and its role in nociception and chronic pain (Sotres-Bayon et al., 2001). As can be observed in Figs. 2 and 3, similar effects and trends on functional connectivity were observed due to the MMT surgery and MMPi treatment between NAcc_L and NAcc_R based

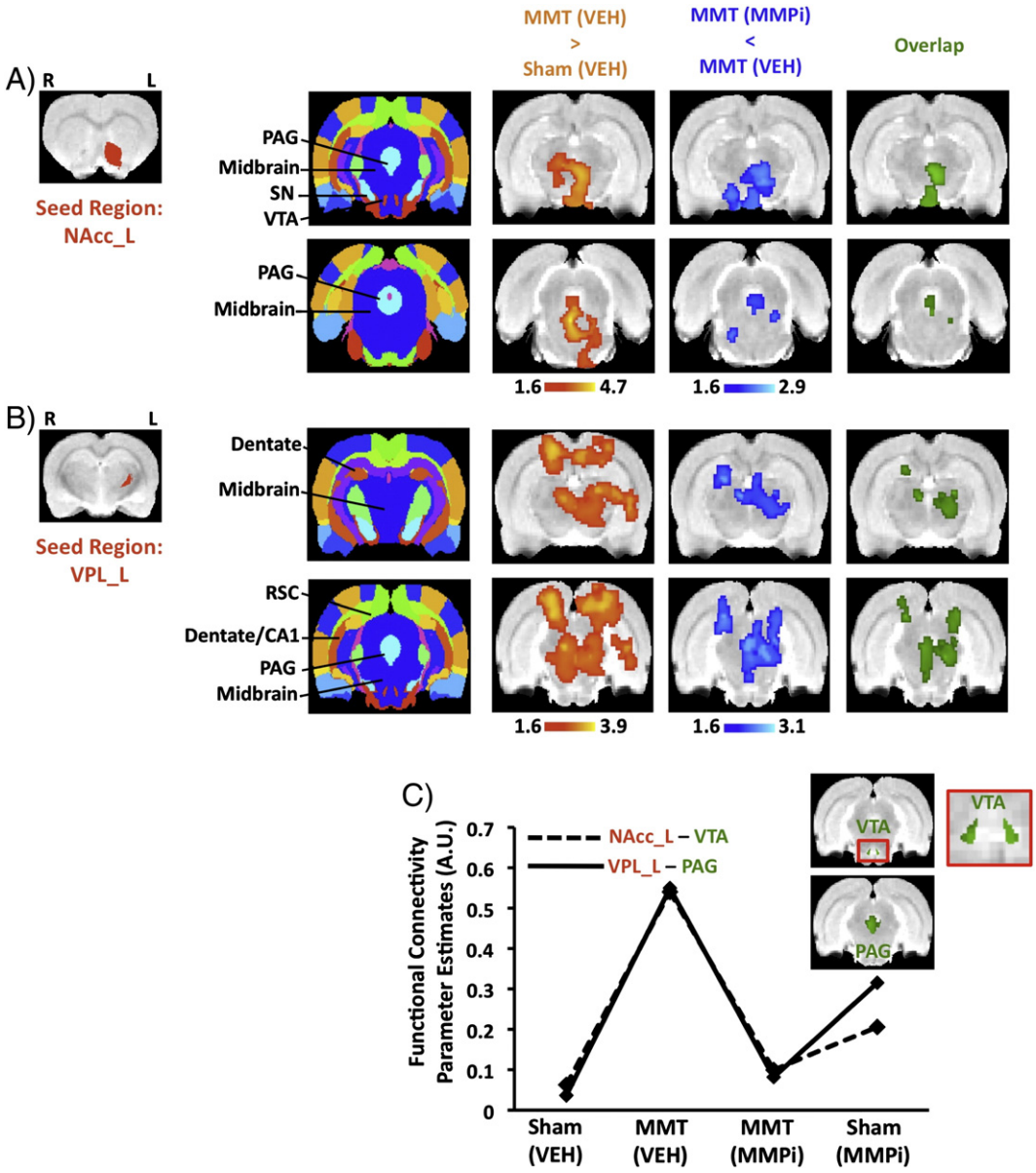

Fig. 2. Suppression of neuroplasticity in the MMT model of osteoarthritis by matrix metalloproteinase inhibition (week 3). NAcc_L (A) and VPL_L (B) based functional connectivity (mixed-effects, group-level results. MMT (VEH) vs. Sham (VEH) comparison revealed hyper-functional connectivity for NAcc_L and VPL_L (orange-yellow regions in left column). MMT (MMPi) vs. MMT (VEH) demonstrated a suppression of the hyper-functional connectivity due to MMPi treatment (blue regions in middle column). Cortical, subcortical and brainstem regions showing both hyper-functional connectivity in the MMT (VEH) cohort and decreased connectivity in the MMT (MMPi) cohort are depicted in the right column (green regions). MMT (VEH)<Sham (VEH) or MMT (MMPi)>MMT (VEH) differences were not statistically significant (see also Supplementary Table 1 for all brain regions with significant activity for NAcc_L and VPL_L based analyses). (C) Graphical representation of functional connectivity across the four experimental cohorts for the NAcc_L-VTA and VPL_L-PAG functional interactions. Effects of the MMT and sham surgery as well as the effect of MMPi treatment can be observed. The line graph also demonstrates a slight increase in functional connectivity between Sham (VEH) and Sham (MMPi) conditions. NAcc, nucleus accumbens; VPL, ventral posterior lateral thalamus; PAG, periaqueductal gray; SN, substantia nigra; VTA, ventral tegmental area; RSC, retrosplenial cortex.

functional connectivity analysis as well as VPL_L and VPL_R based functional connectivity analysis.

When comparing magnitude of effects on functional connectivity resulting from the MMT surgical procedure and MMPi treatment condition between left and right hemisphere seed regions, overall a greater effect throughout the brain was observed for right hemisphere seed regions. For example, for the MMT (VEH)>Sham (VEH) group-level comparison, the number of voxels meeting this criterion for VPL_L and VPL_R was 938 and 1635 voxels, respectively. However, this trend was not constant across all structures. For example, when considering the retrosplenial cortex, the number of voxels meeting the MMT (VEH)>Sham (VEH) criterion for VPL_L and VPL_R was 134 and 77 voxels, respectively. Such differences are likely driven by differences in direct and indirect connectivity patterns between the VPL and other supraspinal structures.

PhMRI infusion response to 3.0 mg/kg IV celecoxib

The mixed-effects, group comparison (vehicle vs. celecoxib) demonstrated a robust attenuation (negative phMRI infusion response relative to vehicle) in supraspinal pain circuitry in MMT animals due to celecoxib (Fig. 4A). This phMRI infusion response was robust in structures such cingulate cortex, periaqueductal gray and thalamus. This effect was particularly strong in bilateral CaPu. A significant potentiation (positive phMRI infusion response relative to vehicle) subsequent to celecoxib administration in the MMT cohort was not

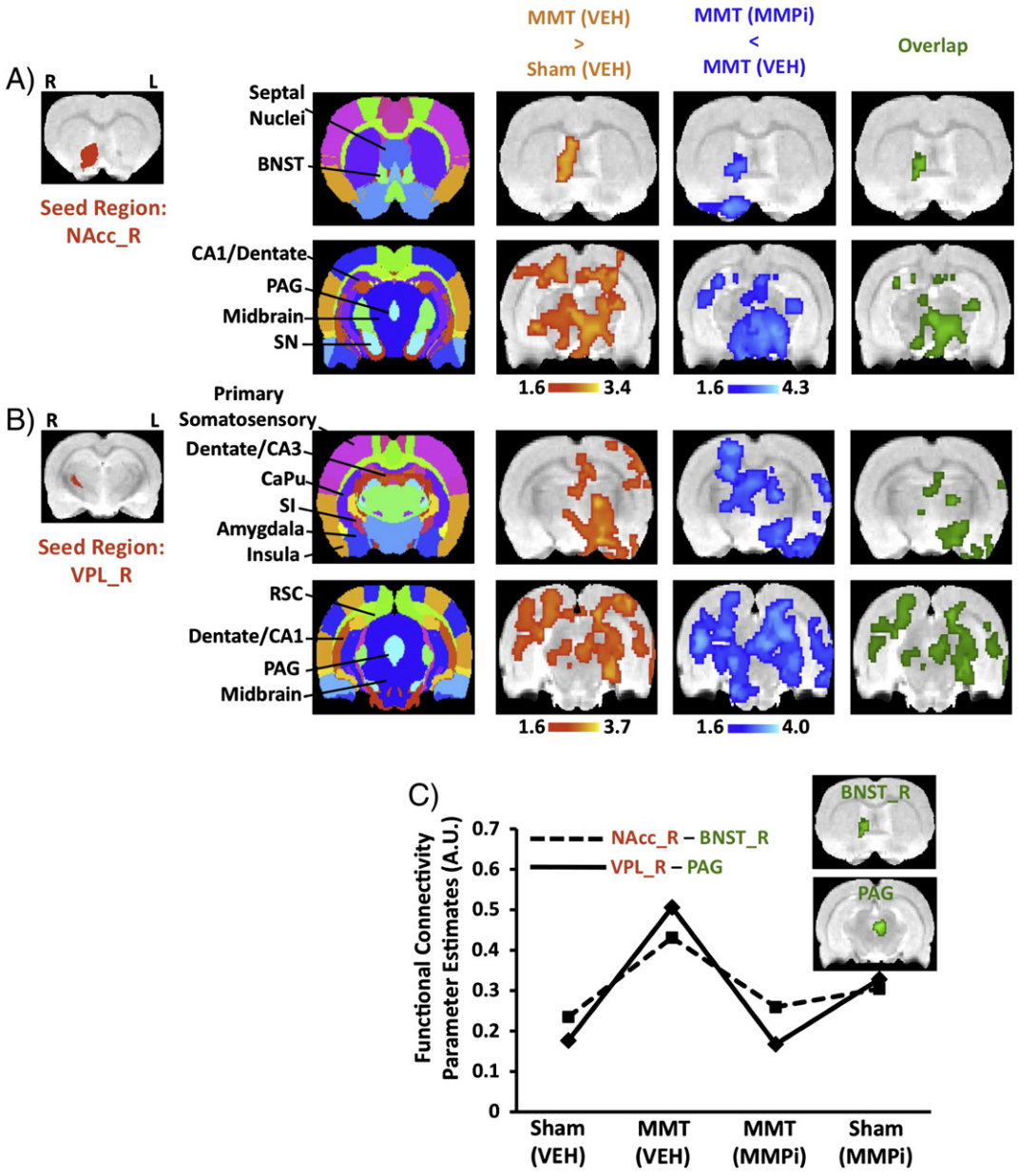

Fig. 3. Suppression of neuroplasticity in the MMT model of osteoarthritis by matrix metalloproteinase inhibition (week 3). NAcc_R (A) and VPL_R (B) based functional connectivity (mixed-effects, group-level results. MMT (VEH) vs. Sham (VEH) comparison revealed hyper-functional connectivity for NAcc_R and VPL_R (orange-yellow regions in left column). MMT (MMPi) vs. MMT (VEH) demonstrated a suppression of the hyper-functional connectivity due to MMPi treatment (blue regions in middle column). Cortical, subcortical and brainstem regions showing both hyper-functional connectivity in the MMT (VEH) cohort and decreased connectivity in the MMT (MMPi) cohort are depicted in the right column (green regions). MMT (VEH)<Sham (VEH) or MMT (MMPi)>MMT (VEH) differences were not statistically significant (see also Supplementary Table 2 for all brain regions with significant activity for NAcc_R and VPL_R based analyses). (C) Graphical representation of functional connectivity across the four experimental cohorts for two example functional interactions (NAcc_R-BNST and VPL_R-PAG). Effects of the MMT and sham surgery as well as the effect of MMPi treatment can be observed. The line graph also demonstrates a slight increase in functional connectivity between Sham (VEH) and Sham (MMPi) conditions. NAcc, nucleus accumbens; VPL, ventral posterior lateral thalamus; BNST, bed nucleus of the stria terminalis; PAG, periaqueductal gray; SN, substantia nigra; SI, substantia innominata; VTA, ventral tegmental area; CaPu, caudate–putamen; RSC, retrosplenial cortex.

observed. In sham animals, the mixed-effects, group comparison (vehicle vs. celecoxib) yielded a slight potentiation of the phMRI infusion response due to celecoxib in regions such as the midbrain (Fig. 4B). Significant attenuation was not detected in the sham cohort.

Characterization of functional connectivity in MMT and sham

Given the robust celecoxib-induced phMRI infusion response observed in the bilateral CaPu in the MMT cohort, the function of the left and right CaPu was separately investigated using seed region functional connectivity analysis (Fig. 5). Moreover, to characterize differences between MMT and sham, independent of drug effect, the 5-min pre-infusion period was assessed. In comparison to the sham condition, the MMT cohort demonstrated an overall increase in CaPu based functional connectivity. The increase in functional connectivity in the brain is noted by the higher intensity regions in the MMT cohort compared to sham. This is true for functional connectivity analysis where either the left or right CaPu was used as the seed region.

Effects of 3.0 mg/kg IV celecoxib on functional connectivity

Administration of 3.0 mg/kg IV celecoxib in the MMT animals significantly decreased functional connectivity between the CaPu and

Table 1
ANOVA analysis of functional connectivity.

Functional interaction	$F_{3,\ 18}$	*p*-value
NAcc_L-VTA	3.238	0.046
NAcc_L-PAG	0.783	0.519
NAcc_R-VTA	7.612	0.002
NAcc_R-PAG	5.288	0.009
NAcc_R-BNST_R	1.392	0.277
VPL_L-PAG	4.438	0.017
VPL_L-S1	0.928	0.447
VPL_R-PAG	6.930	0.003
VPL_R-S1	3.132	0.051

F-Critical-3.16; NAcc, nucleus accumbens; VTA, ventral tegmental area; PAG, periaqueductal gray; BNST, bed nucleus of the stia terminalis; S1, primary somatosensory cortex.

several regions within CNS pain circuitry (i.e., nucleus accumbens, thalamus, hippocampus (CA1, CA3 and dentate) and PAG (Fig. 5). For this functional connectivity analysis, the last 5 min of the phMRI scan was used as this time interval corresponded to the longest duration of celecoxib exposure. Functional connectivity changes were particularly robust in the MMT cohort when the left CaPu was used as a seed region, while little or no change in functional connectivity between vehicle and celecoxib condition was observed in the sham cohort. The attenuation of increased functional connectivity in the MMT cohort by acute celecoxib administration was similar to the pharmacodynamic effects on functional connectivity by chronic MMPi treatment. Also, the network of structures affected by both celecoxib and MMPi treatment conditions was similar (i.e., nucleus accumbens, CaPu, thalamus, hippocampus, amygdala, PAG and midbrain) (Fig. 6).

Consistency of celecoxib-induced pharmacodynamic effects in the MMT model

We sought to determine the consistency of phMRI infusion responses and seed region functional connectivity changes elicited by celecoxib in the MMT rats. A conjunction analysis of 2 distinct cohorts ($n = 6$/cohort) of MMT animals demonstrated a consistent negative phMRI infusion response to celecoxib in regions such as CaPu (Fig. 7A). This effect can be observed in the group-level statistical maps as well as at the single-subject level. A conjunction analysis of left hemisphere, CaPu based functional connectivity demonstrated consistent decrease in functional connectivity at the group-level and also at the single-subject level (Fig. 7B). Consistent decreases in functional connectivity were observed between the left CaPu and CNS pain circuitry regions such as the VPL and PAG. It is noted that different experimenters performed data collection of the two distinct cohorts. All other experimental procedures including animal vendor, housing of animals, personnel performing surgical procedures and data analysis were constant between the two cohorts.

Effects of the MMT surgery and MMPi treatment on the knee joint

To assess joint trauma as determined by cartilage degradation, histological assessment of the effects of the MMT surgery with MMPi treatment was also performed in an independent experiment (Fig. 8A–D). Similar to the imaging study, tissue collection for histological assessment was performed 3 weeks post-surgery. In comparison to the sham condition, substantial articular cartilage degradation and fibrillation were observed in the MMT (VEH) condition (Fig. 8B). Importantly, MMPi treated animals exhibited a significant ($p<0.001$, one-way ANOVA, Tukey's post-hoc test) reduction in cartilage pathology as compared to the MMT (VEH) group (Fig. 8C and D).

Using gadolinium-enhanced MRI, the effects of the MMT surgery on the knee joint were qualitatively assessed in animals undergoing functional brain imaging (Fig. 8E). In Fig. 8E, a representative image of the MMT knee joint obtained from gadolinium-enhanced MRI depicts structural abnormalities at various locations in the knee joint (i.e., cartilage or subchondral bone). Similar effects in the joint were not obtained in the sham knee. The structural changes observed in the MMT knee joint are consistent with previous findings (Wang, 2008; Xie et al., 2010). These results confirmed knee joint trauma following MMT surgical procedures. Efforts to utilize preclinical MRI to evaluate pharmacological effects on knee joint trauma in the MMT model are currently ongoing.

Discussion

Summary of findings

The current preclinical data indicate that induction of a chronic osteoarthritic state can modulate the function of motivational, reward-aversion and sensory components of pain mediating circuitry in the brain. In *Part I*, we have demonstrated for the first time how predominately peripheral MMP inhibition by MMPi can suppress knee joint trauma as well as mediate functional connectivity changes in supraspinal pain circuitry in the MMT model of osteoarthritis. Subsequently, we characterized celecoxib-induced pharmacodynamic

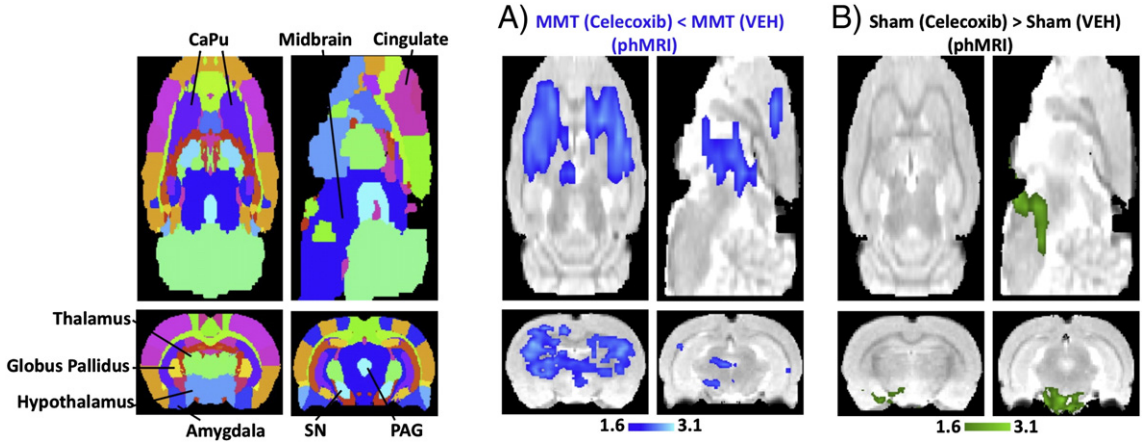

Fig. 4. PhMRI infusion responses to 3.0 mg/kg IV celecoxib (week 5). (A) A group comparison (vehicle vs. celecoxib) demonstrated a robust negative phMRI infusion response relative to vehicle in CNS pain circuitry in MMT animals due to celecoxib administration. The negative phMRI infusion response was particularly robust in the bilateral CaPu (see also Fig. 7). In Supplemental Fig. 1, time course data from the MMT celecoxib condition has been given. (B) In sham animals, the mixed-effects, group comparison (vehicle vs. celecoxib) yielded a positive celecoxib phMRI infusion response relative to vehicle in region such as the midbrain. In MMT and sham cohorts, some phMRI activity is more profound in one hemisphere than the other. This effect may stem from the unilateral nature of the surgical procedures. CaPu, caudate–putamen; PAG, periaqueductal gray; SN, substantia nigra.

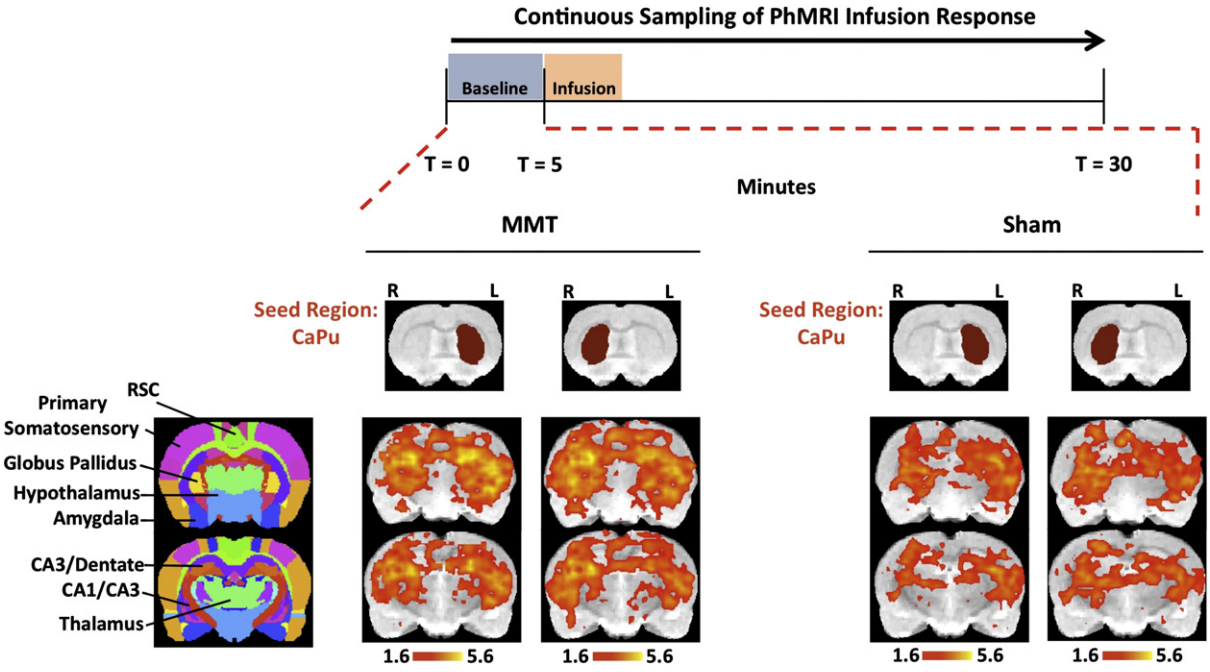

Fig. 5. CaPu based functional connectivity in MMT and sham surgical animals (week 5). To further characterize the MMT model with respect to sham, as well as characterize the function of the CaPu in the MMT model, a seed region CaPu functional connectivity analysis was performed. For this analysis, the 5-min pre-infusion or baseline period of phMRI scans from all animals (MMT and sham) and both vehicle and celecoxib was used. The within-group, mixed-effects analysis demonstrated an overall increase in functional connectivity, as determined by higher intensity regions, in the MMT cohort compared to sham cohort. The red dashed lines indicate that the functional connectivity results pertain only to the pre-infusion period. NAcc, nucleus accumbens; CaPu, caudate–putamen; PAG, periaqueductal gray; SN, substantia nigra; VTA, ventral tegmental area.

activity within supraspinal circuitry in MMT animals in *Part II* of the study. Celecoxib yielded robust decreases in phMRI activity in the MMT cohort, particularly in structures such as the bilateral CaPu. Following celecoxib treatment, a significant decrease in functional connectivity was observed between the CaPu and structures such as NAcc, thalamus (VPL), hippocampus and PAG, a finding similar to that observed in *Part I* of this study where pharmacodynamic effects MMPi were evaluated. Importantly, the robust decreases in phMRI activity as well as CaPu based functional connectivity were specific to the MMT model of osteoarthritis, and were consistently observed across two distinct MMT populations. The findings related to MMPi and celecoxib are of particular importance given that these compounds are not suitable for a PET or single photon emission computed tomography (SPECT) based appraisal, where target engagement and receptor occupancy is assessed. Such a situation is common for many pain and immunology targets (i.e., COX-2 or PGE_2). Therefore, functional connectivity and phMRI based methodologies may be of particular utility in cases where a suitable radioactive ligand is unavailable; however, a mechanistic based evaluation in the brain for a marketed or novel compound is desired (Jenkins, 2012).

The role of NAcc, VPL and CaPu in pain

The MMT-induced supraspinal neuroplasticity and MMPi treatment effects were assessed by characterizing the functional connectivity of the NAcc and VPL. The NAcc seed region was chosen given its previously established role in motivational, reward-aversion and emotional appraisal aspects of pain processing and downstream modulation of pain (Baliki et al., 2010; Becerra et al., 2001; Gear et al., 1999; Zubieta et al., 2001). Furthermore, the NAcc has been shown to be particularly predictive of pain in humans (Baliki et al., 2010), and subjected to morphological changes under distinct pain states (Gustin et al., 2011; Wartolowska et al., 2012). Baliki et al. recently reported strong connectivity between NAcc and structures such as medial prefrontal cortex (mPFC), thalamus, CaPu and PAG. The NAcc-mPFC functional connectivity in particular was positively correlated with ratings of pain intensity as well as distinguished patients with chronic back pain from healthy controls. In comparison to healthy subjects, fibromyalgia patients not only showed a reduced level of mu-opioid receptor binding potential in the NAcc, but also, the binding potential was negatively correlated with affective measures of pain reported by patients (Harris et al., 2007). These clinical observations strongly support the notion that properties of the NAcc, which include NAcc hyper-connectivity in patients, reflect and underlie ongoing pain.

The VPL, on the other hand, is a critical component of the ascending pain pathway that relays sensory and discriminative aspects of nociceptive stimulus to cortical structures such as somatosensory and insular cortices (Chung et al., 1986; Kenshalo et al., 1980). Recent preclinical neuroimaging studies evaluating a neuropathic pain state have demonstrated that modulation of functional activity in the thalamus can be elucidated during acute pain stimulation, an acute gabapentin challenge or both (Governo et al., 2008; Takemura et al., 2011). Thalamic activity in healthy human subjects undergoing thermal pain has been shown to be parametrically related to the properties of the noxious stimuli as well as to subjective pain ratings (Coghill et al., 1999; Upadhyay et al., 2011a). Recent studies by Napadow et al. (2010, 2012) in fibromyalgia and Cauda et al. (2009) in diabetic neuropathic pain have identified increased thalamic connectivity with pain modulating regions such as the insula and dorsolateral prefrontal cortex in these patients. Along similar lines, reduced thalamic–midbrain connectivity was shown to be associated with improved pain affect during heat allodynia in healthy volunteers (Lorenz et al., 2003). With respect to thalamic morphology, Gustin et al. (2011) and Gwilym et al. (2010) have demonstrated decreases in thalamic volume in trigeminal neuropathic pain and hip osteoarthritis patients, respectively. In the case of hip osteoarthritis patients, the decrease in thalamic volume was reversed subsequent to arthroplasty. Taken together, increased NAcc and thalamic functional connectivity with other pain-related brain areas and volumetric changes of these two subcortical structures may reflect or be components of brain signatures of ongoing pain. These recent functional and

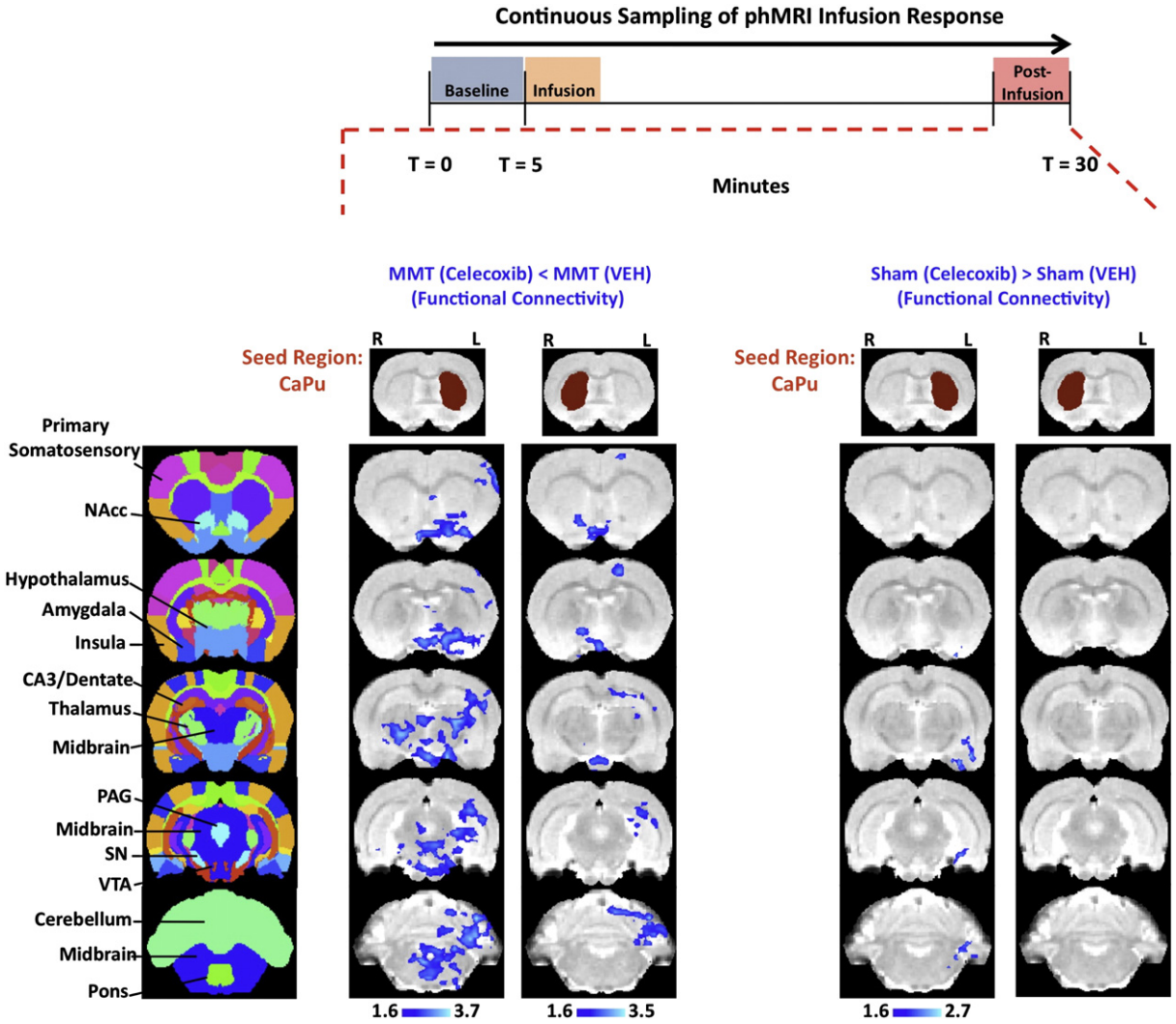

Fig. 6. Effects of celecoxib on CaPu based functional connectivity (week 5). Administration of 3.0 mg/kg IV celecoxib in the MMT animals significantly decreased functional connectivity between the CaPu and several regions within the CNS pain circuitry (i.e., NAcc, thalamus, hippocampus (CA1, CA3 and dentate) and PAG). For this functional connectivity analysis, the last 5 min of phMRI scan was utilized. Functional connectivity changes were particularly robust in the MMT cohort when CaPu_L was used as a seed region. Little or no change in functional connectivity between vehicle and celecoxib conditions was observed in the sham cohort. The red dashed lines indicate that the functional connectivity results pertain only to the post-infusion period. NAcc, nucleus accumbens; CaPu, caudate–putamen; PAG, periaqueductal gray; SN, substantia nigra; VTA, ventral tegmental area.

structural imaging-based findings observed in various clinical pain populations help to further define the neuroplasticity induced by a chronic pain state (Seifert and Maihofner, 2011).

The phMRI and functional connectivity readouts reported in this study strongly suggest that the CaPu is robustly affected by the pharmacological action for celecoxib, and is also a structure whose function is altered under the MMT model condition. Similar to the NAcc, the CaPu is a structure of the greater basal ganglia network. With respect to its structural connectivity, the CaPu possesses direct and indirect projections (efferent and afferent) to the cortex, subcortical structures such as the thalamus, hippocampus and amygdala and also, other basal ganglia structures (Cohen et al., 2009; Voorn et al., 2004). From a functional perspective, the dorsal striatum overall is implicated in sensation, motor function, reward-aversion and salience, all of which are key aspects of pain processing (Barker, 1988; Borsook et al., 2010; Chudler and Dong, 1995; Upadhyay et al., 2011a). In recent preclinical imaging work in anesthetized rodents, it has been demonstrated that acute noxious forepaw stimulation (electrical or mechanical) induces a magnitude-dependent response in the bilateral CaPu as determined by either cerebral blood volume or BOLD fMRI signal changes (Shih et al., 2009; Zhao et al., 2012). As demonstrated by Shih et al. the evoked pain response in the CaPu can be significantly reduced by eticlopride, suggesting that CaPu activity during a pain state is driven in part by dopamine D2 receptor activity. Interestingly, studies by Shih et al. and Zhao et al. both demonstrated that the response to noxious stimulation measured in the CaPu was anti-correlated with that measured in primary somatosensory cortex. In the current investigation, not only was an increase in functional connectivity observed between the CaPu and primary somatosensory cortex, but also, chronic MMPi treatment mitigated this increase. Thus, the previous and current functional imaging results further suggest an important role for the CaPu-somatosensory cortex functional interaction during pain processing.

Given the known connectivity of the caudate–putamen and its role in multiple aspects of pain, this structure likely plays an important role in integrating information specific to nociceptive and neuropathic pain. Furthermore, in addition to the sensitization present in the MMT condition (Bove et al., 2006), behavioral changes involving proprioception or joint protection during movement could also lead to changes in caudate–putamen function given this structure's important role in movement and sensorimotor processing. In turn, functional changes elicited by changed proprioception or locomotion may be uniquely affected by a pharmacological compound (i.e., acutely administered celecoxib). It is important to note that the current datasets do not

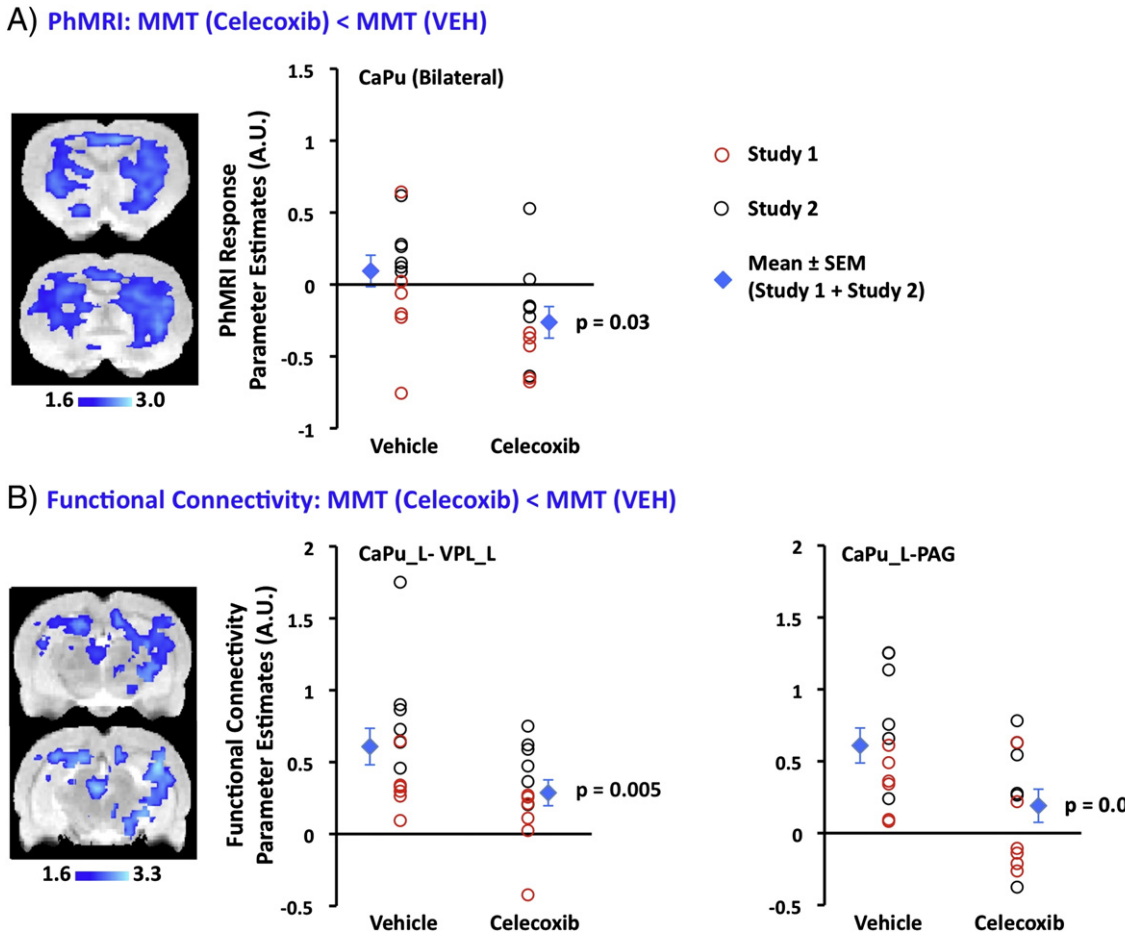

Fig. 7. Consistent PhMRI and functional connectivity changes induced by celecoxib in the MMT model of OA (week 5). (A) A conjunction analysis of 2 distinct cohorts ($n = 6$/cohort) of MMT animals demonstrated a consistent negative phMRI infusion response to celecoxib in CNS regions such as CaPu. This effect can be observed in the group-level statistical maps as well as at the single-subject level. (B) A conjunction analysis of CaPu based functional connectivity demonstrated a consistent decrease in functional connectivity at the group-level and also at the single-subject level. Consistent decreases in function connectivity were observed between the left CaPu and CNS pain circuitry regions such as the ventral lateral thalamus and periaqueductal gray. Single-subject parameter estimate specific to the phMRI and functional connectivity results were extracted from the full ROI defined by the in-house atlas. Two-tailed *t*-tests were used to determine group-level statistical significance reported in each scatter plot. CaPu, caudate–putamen; VPL, ventral posterior lateral thalamus; PAG, periaqueductal gray.

enable a straightforward differentiation between effects solely driven by a sustained pain state or altered proprioception or locomotion. This is particularly the case since pain and movement processing can be and are tightly coupled.

MMP inhibition

MMPi has potency for MMP-2, MMP-9 and MMP-13 (Gum et al., 2001; Wada et al., 2002), all of which play a key role in the cartilage degradation process (Billinghurst et al., 1997; Heathfield et al., 2004). For example, it has been shown that in a surgically induced osteoarthritis model, MMP-13 knockout mice demonstrated less cartilage degradation than wild-type mice (Little et al., 2009). This preclinical finding is important given that MMP-13 is known to cleave type II collagen, the principal extracellular matrix protein for articular hyaline cartilage. Other MMPs, such as MMP-2 and MMP-9, digest type I collagen as well as aggrecan, each of which is present in cartilage tissue (Fosang et al., 1992; Nguyen et al., 1993). Importantly, activities of MMP-2 and MMP-9 are both up-regulated in the joints of osteoarthritis patients. Given the broad-spectrum nature of MMPi in conjunction with the known role of multiple MMPs in an osteoarthritis disease state, the disease-modifying osteoarthritis drug effect of MMPi observed in the MMT knee joint is driven by inhibition of multiple MMPs. Moreover, to further determine how broad-spectrum MMP inhibition can affect joint trauma, evaluation of other peripheral pathological conditions relevant to osteoarthritis such as osteophyte formation or changes in the subchondral bone may be beneficial in future investigation.

In the basal rat nervous system, MMPs have a low expression level (Yong et al., 2001). In the rat brain specifically, MMP-13, for which MMPi has potency, comprises of ~3% of the total MMP concentration. This is very low in comparison to MMP-24, which makes up for ~60% of the total MMP concentration (Sekine-Aizawa et al., 2001). In the case of a central nervous system diseased state, notably multiple sclerosis (Gijbels et al., 1992; Waubant et al., 1999) and brain ischemia (Romanic et al., 1998; Rosenberg et al., 1996), the activity of MMPs such as MMP-2, MMP-7 and MMP-9 is up-regulated. Preclinical models of drug dependence, Alzheimer's disease and epilepsy have shown involvement of MMP-2 and MMP-9 (Mizoguchi et al., 2011), while MMP-9 has been linked to normally occurring neuroplasticity that is not pathologic in nature (Michaluk et al., 2011). With respect to pain, Kawasaki and colleagues have recently demonstrated involvement of MMP-2 and MMP-9 in the spinal nerve ligation model (Ji et al., 2009; Kawasaki et al., 2008), a model of neuropathic pain. Also, spinal MMP-3 activity has been linked to the inflammatory hypersensitivity observed in the carregeenan model (Christianson et al., 2012). It can be considered that the possible presence and effects of peripheral nerve injury in the MMT condition could propagate to the brain and induce neuroplasticity in supraspinal circuitry mediating pain. Thus, in

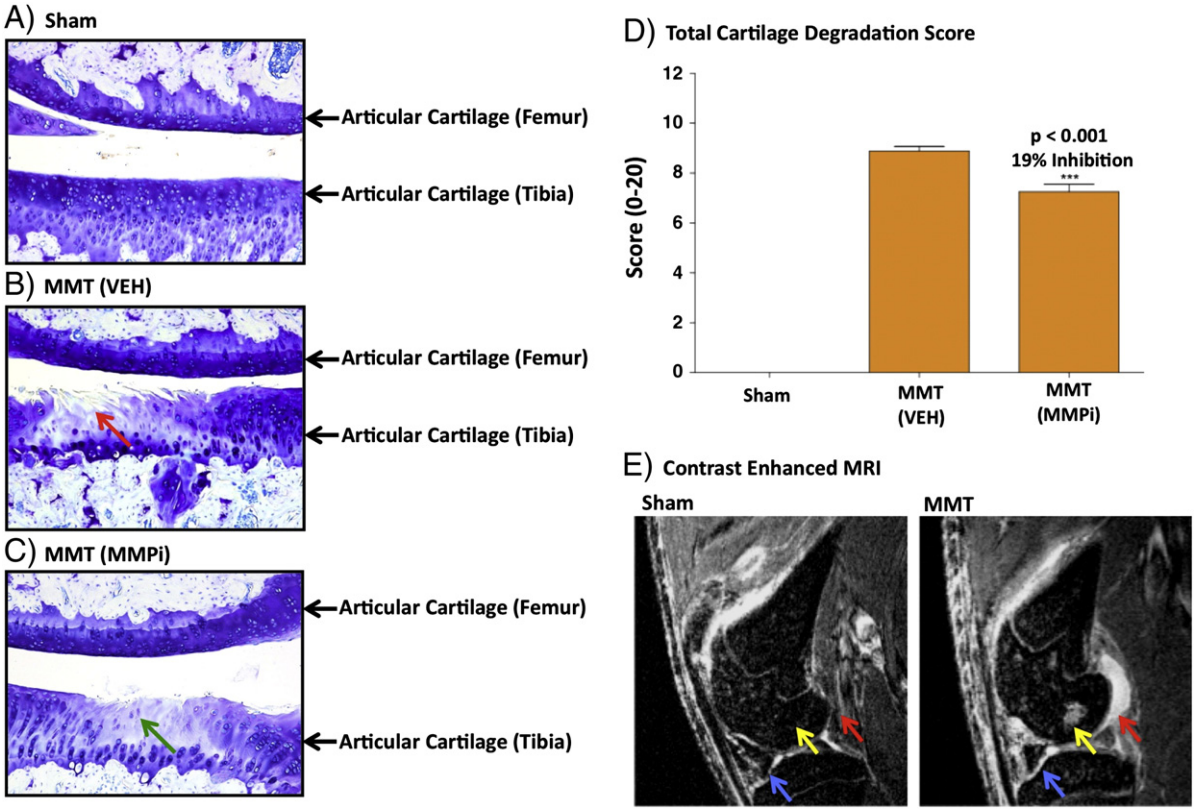

Fig. 8. Inhibition of cartilage degradation in the MMT model of osteoarthritis by matrix metalloproteinase inhibition (week 3). In a separate study, the effects of the MMT surgery and MMPi treatment on articular knee cartilage of male Lewis rats were assessed using histology (toluidine-blue staining) 3 weeks post-surgery. Drug administration of the histology study was similar to that of the brain imaging study (3 weeks of 30 mg/kg MMPi PO BID dosing or 3 weeks of VEH PO BID dosing starting at day of MMT or sham surgical procedures). Representative toluidine-blue stained frontal cross-sections from the medial femorotibial joints from sham (A), (MMT (VEH) (B) and MMT (MMPi) (C) treated animals are shown. In comparison to the Sham condition, MMT (VEH) shows substantial cartilage degradation in the tibial articular cartilage (red arrow) as well as fibrillation. These histological findings are in accord with previous studies evaluating the MMT model (Bove et al., 2006). The MMT (MMPi) conditions shows less cartilage degradation (green arrow) in the tibial articular cartilage indicating a slowing of the osteoarthritis-like disease state. A graphical representation of the effects of the MMT surgery and MMPi treatment are shown in (D). Statistical analysis was performed using a one-way ANOVA, Tukey's post-hoc test. $^{***}p<0.001$. (E) Structural assessment of the sham (A) and MMT (B) knee was accomplished using gadolinium-enhanced MRI at week 3 post-surgery. Here abnormalities in the representative MMT knee can be observed within the bone-soft tissue interface (red arrow), subchondral bone (yellow arrow) and cartilage area (blue arrow). Such abnormalities, specifically hyper-intensities, are not present in the sham knee.

addition to the effects of MMPi on articular cartilage, peripheral inhibition of MMP-2, MMP-3 and MMP-9 by MMPi at the nerve injury site may also have indirectly reduced neuroplasticity in the MMT (MMPi) cohort. It is noted that a limitation of this study was the inability to distinguish to what degree peripheral MMPi action on articular cartilage degradation or peripheral nerve injury each contributed to subsiding changes in supraspinal pain circuitry in MMT animals.

MMPi levels in brain and spinal cord tissue were very low in comparison to levels measured in plasma. At 3 weeks following 30 mg/kg MMPi PO BID dosing, brain and spinal cord-to-plasma ratios were 0.08 and 0.06, respectively. MMPi has properties of a substrate of P-gp and this may explain why MMPi levels at least in the brain were very low. Given that tissue perfusion was not performed in the PK studies, the MMPi levels detected in the brain and spinal cord had contributions from vasculature in these two types of tissues. Thus, MMPi levels in brain and spinal cord tissue are slightly less than those reported. We speculate that it is possible that the very modest levels of MMPi in brain and spinal cord or a metabolite of this compound could directly have some affect on brain function. It is worth noting that within the Sham (MMPi) condition, a slight increase in functional connectivity relative to the Sham (VEH) condition was observed (Figs. 2C and 3C), which supports the plausibility of direct central action of MMPi or a metabolite of MMPi. Nonetheless, the significant inhibition of neuroplasticity in conjunction with the inhibition of cartilage degradation observed in the MMT model of osteoarthritis strongly suggests that the main effects of MMPi are peripheral in nature.

In rodents and humans, chronic and periodically re-occurring pain states have been shown to alter neuro-sensory pain pathways as well as the overall structure of the CNS itself (Porro, 2003; Rodriguez-Raecke et al., 2009; Seminowicz et al., 2009; Tu et al., 2010). There is ongoing debate as to whether such alterations are causal, resultant, or incidental. We cannot therefore rule out the possibility that CNS alterations such as these, which may or may not occur, following MMT surgery contributed to the results. Despite the lack of MMPi blood–brain barrier penetration and the inhibition of cartilage degradation in MMPi treated animals, the changes in functional connectivity in the present study could be mediated via structural modulation within the brain during the chronic pain state.

Selective COX-2 inhibition

Inhibition of COX-2 and PGE_2 has been linked to activity with opioid, dopaminergic, glutamatergic and GABAergic neurotransmitter systems (Cashman, 1996) of which the CaPu is a component (Voorn et al., 2004). Franca et al. (2006) suggested that the analgesic effect induced by inhibition of COX-2 is driven by endogenous opioids, while Rezende et al. (2009) demonstrated that hypoanalgesia obtained by centrally administered celecoxib in a peripheral inflammatory pain model could be reversed by naltrexone, a μ- and κ-opioid receptor antagonist. Interestingly, in the current study, a decrease in functional connectivity between the CaPu with the thalamus and somatosensory cortex was observed as a result of celecoxib treatment. Similar changes in functional connectivity have been observed resulting from partial

agonist action at the μ-opioid receptor site (Upadhyay et al., 2010). The interaction between COX-2 mediated events and the opioid system may underlie why the two mechanism of actions (MOAs) have similar effects on functional connectivity. Based on correlation between PGE_2 synthesis and glutamate release, COX-2 inhibition may also affect the glutamatergic system (Bezzi et al., 1998). Moreover, in a preclinical Parkinson's disease model, COX-2 inhibition by celecoxib was observed to mitigate the loss of dopamine cell loss in the striatum (Sanchez-Pernaute et al., 2004). These studies suggest a strong crosstalk between various neurotransmitter systems implicated in pain processing with COX-2 and PGE_2 activity. This pharmacological crosstalk in conjunction with the known functional properties of the CaPu may explain the celecoxib-induced phMRI infusion responses and caudate–putamen based functional connectivity changes measured in this study. To determine the extent to which selective COX-2 inhibition interacts with a specific neurotransmitter system, a phMRI study involving two pharmacological treatments may be performed in future studies (Chin et al., 2011). Importantly, such a pharmacological imaging study could be performed in the MMT model or in a clinical setting involving osteoarthritis patients.

In the brain, up-regulation of COX-2 by interleukin-1 also yields central sensitization or a state of hypersensitivity to pain (Samad et al., 2001). Such results from earlier studies may help explain how functional properties (i.e., functional connectivity) of the brain are altered in the MMT model relative to the sham condition, and why a robust response to celecoxib treatment is detected as determined by phMRI and functional connectivity measures. For example, it is plausible that neuronal hyper-excitability in the CaPu under the MMT condition may be mitigated by administration of celecoxib. However, what cannot be determined exactly with the implemented imaging methodology is whether the effects observed in the CaPu are due to direct pharmacological action on this structure by celecoxib, indirect pharmacological action stemming from the periphery and other brain structures or a combination of the two.

Implementation of translation pain imaging in osteoarthritis

In the current investigation, MMT animals relative to the sham animals were characterized as having increased connectivity amongst structures that mediate various aspects of pain (i.e., NAcc, VPL, CaPu, PAG, hippocampus and somatosensory cortex). The increases in functional connectivity currently demonstrated in MMT animals in conjunction with those previously observed in pain patients further suggest that assessment of functional connectivity in general may provide a much needed conduit between preclinical and clinical investigations where pain and potential analgesics are assessed. Evaluation of supraspinal functional and structural properties of the brain in preclinical and clinical imaging studies can provide an objective measure that can be used in conjunction with traditional pharmacokinetic and behavioral readouts (i.e., spinal reflex responses in rodents and highly variable subjective pain ratings in humans). By implementing such an imaging-based approach, an opportunity exists where back-translation of findings is possible. The latter is true and important whether a pharmacological compound under clinical evaluation has analgesic efficacy or not, and a feature not available when using only the traditional behavioral preclinical and clinical endpoints. It is noted that a preclinical functional imaging-based evaluation of pharmacological compounds is only one possible manner in which to better identify treatments for osteoarthritis pain. For example, Okun et al. (2012) have investigated the monosodium iodoacetate (MIA) model of osteoarthritis under various treatment conditions in a condition place preference paradigm. More recently, Andrews et al. (2012) have investigated natural burrowing behaviors in preclinical models of pain, and the effects of gabapentin and ibuprofen on such behaviors. Perhaps a combination of functional imaging-based endpoints and alternative behavioral assessments can provide a more thorough preclinical screen of compounds prior to their clinical assessment.

Study limitations

There are limitations to the utilization of functional connectivity and other functional imaging-based measures as translational endpoints in preclinical and clinical investigations. In studies such as the current one, a preclinical model (i.e., MMT model) and pharmacological compound (MMPi) is evaluated within a 3-week period following surgical induction of osteoarthritis and under an anesthetized state (all MMT and sham animals were scanned under 2% isoflurane). It is known that presence of an anesthetic affects brain function (Boveroux et al., 2010); however, it is unknown if the presence of anesthesia would always significantly hinder a model characterization and pharmacological effect from being elucidated. The results of this preclinical investigation suggest a case where anesthesia was present, but did not hinder the study hypothesis from being tested. It can be easily realized that this preclinical condition is different from that which is commonly the case in an osteoarthritis clinical study, where patients are in a chronic pain state (pain that last for more than three months), may have differences in the etiology (e.g., induction of osteoarthritis), suffer from other co-morbidities, and may have differences in functional and structural properties of the brain due to long-term use of prescription medication. Of course, intrinsic differences in brain structural and functional properties exist between rodents and humans, and this may be reflected in functional connectivity, yet even very fundamental networks in the human brain such as the default-mode network have been preserved in large part within the rodent brain under awake and anesthetized conditions (Lu et al., 2012; Upadhyay et al., 2011b). Nonetheless, to better understand how such limitations impact the translatability of functional imaging-based readouts relevant to osteoarthritic pain, further clinical imaging work involving osteoarthritis patients and pharmacological compounds are necessary.

Conclusion

The current investigation provides evidence of increases in supraspinal functional connectivity amongst brain regions implicated in pain processing in a preclinical surgical model of osteoarthritis. A novel disease-modifying osteoarthritis drug with peripheral (broad-pectrum, matrix metalloproteinase inhibition) as well as a peripherally and centrally acting mechanism of action (selective COX-2 inhibition) was shown to affect the function of supraspinal networks in an osteoarthritic state. The observation of these aberrant connectivity patterns as well as their pharmacological modulation suggests that a potential translatable pharmacodynamic biomarker relevant to osteoarthritic pain may be obtained with functional imaging.

Supplementary data to this article can be found online at http://dx.doi.org/10.1016/j.neuroimage.2012.08.084.

Disclosure

Abbott Laboratories financially supported the current study. All authors of the manuscript are full-time employees of Abbott Laboratories and have no other competing financial interest to declare.

Acknowledgments

The authors would like to thank Tiffany Garrison, Mira Hinman and David Calderwood for helpful discussion during the preparation of this manuscript. Todd Howard, Tricia Rinaldo and Michael McNally assisted in animal dosing and care. Hongyu Xu and Donna Strasburg assisted with pharmacokinetic studies.

References

Andrews, N., Legg, E., Lisak, D., Issop, Y., Richardson, D., Harper, S., Pheby, T., Huang, W., Burgess, G., Machin, I., Rice, A.S., 2012. Spontaneous burrowing behaviour in the rat is reduced by peripheral nerve injury or inflammation associated pain. Eur. J. Pain 16, 485–495.

Baliki, M.N., Geha, P.Y., Fields, H.L., Apkarian, A.V., 2010. Predicting value of pain and analgesia: nucleus accumbens response to noxious stimuli changes in the presence of chronic pain. Neuron 66, 149–160.

Barker, R.A., 1988. The basal ganglia and pain. Int. J. Neurosci. 41, 29–34.

Becerra, L., Breiter, H.C., Wise, R., Gonzalez, R.G., Borsook, D., 2001. Reward circuitry activation by noxious thermal stimuli. Neuron 32, 927–946.

Bezzi, P., Carmignoto, G., Pasti, L., Vesce, S., Rossi, D., Rizzini, B.L., Pozzan, T., Volterra, A., 1998. Prostaglandins stimulate calcium-dependent glutamate release in astrocytes. Nature 391, 281–285.

Billinghurst, R.C., Dahlberg, L., Ionescu, M., Reiner, A., Bourne, R., Rorabeck, C., Mitchell, P., Hambor, J., Diekmann, O., Tschesche, H., Chen, J., Van Wart, H., Poole, A.R., 1997. Enhanced cleavage of type II collagen by collagenases in osteoarthritic articular cartilage. J. Clin. Invest. 99, 1534–1545.

Borsook, D., Upadhyay, J., Chudler, E.H., Becerra, L., 2010. A key role of the basal ganglia in pain and analgesia–insights gained through human functional imaging. Mol. Pain 6, 27.

Bove, S.E., Laemont, K.D., Brooker, R.M., Osborn, M.N., Sanchez, B.M., Guzman, R.E., Hook, K.E., Juneau, P.L., Connor, J.R., Kilgore, K.S., 2006. Surgically induced osteoarthritis in the rat results in the development of both osteoarthritis-like joint pain and secondary hyperalgesia. Osteoarthr. Cartil. 14, 1041–1048.

Boveroux, P., Vanhaudenhuyse, A., Bruno, M.A., Noirhomme, Q., Lauwick, S., Luxen, A., Degueldre, C., Plenevaux, A., Schnakers, C., Phillips, C., Brichant, J.F., Bonhomme, V., Maquet, P., Greicius, M.D., Laureys, S., Boly, M., 2010. Breakdown of within- and between-network resting state functional magnetic resonance imaging connectivity during propofol-induced loss of consciousness. Anesthesiology 113, 1038–1053.

Breder, C.D., Dewitt, D., Kraig, R.P., 1995. Characterization of inducible cyclooxygenase in rat brain. J. Comp. Neurol. 355, 296–315.

Cashman, J.N., 1996. The mechanisms of action of NSAIDs in analgesia. Drugs 52 (Suppl. 5), 13–23.

Cauda, F., Sacco, K., Duca, S., Cocito, D., D'Agata, F., Geminiani, G.C., Canavero, S., 2009. Altered resting state in diabetic neuropathic pain. PLoS One 4, e4542.

Chaplan, S.R., Bach, F.W., Pogrel, J.W., Chung, J.M., Yaksh, T.L., 1994. Quantiative assessment of tactile allodynia in the rat paw. J. Neurosci. Methods 53, 55–63.

Chin, C.L., Upadhyay, J., Marek, G.J., Baker, S.J., Zhang, M., Mezler, M., Fox, G.B., Day, M., 2011. Awake rat pharmacological magnetic resonance imaging as a translational pharmacodynamic biomarker: metabotropic glutamate 2/3 agonist modulation of ketamine-induced blood oxygenation level dependence signals. J. Pharmacol. Exp. Ther. 336, 709–715.

Christianson, C.A., Fitzsimmons, B.L., Shim, J.H., Agrawal, A., Cohen, S.M., Hua, X.Y., Yaksh, T.L., 2012. Spinal matrix metalloproteinase 3 mediates inflammatory hyperalgesia via a tumor necrosis factor-dependent mechanism. Neuroscience 200, 199–210.

Chudler, E.H., Dong, W.K., 1995. The role of the basal ganglia in nociception and pain. Pain 60, 3–38.

Chung, J.M., Lee, K.H., Surmeier, D.J., Sorkin, L.S., Kim, J., Willis, W.D., 1986. Response characteristics of neurons in the ventral posterior lateral nucleus of the monkey thalamus. J. Neurophysiol. 56, 370–390.

Ciceri, P., Zhang, Y., Shaffer, A.F., Leahy, K.M., Woerner, M.B., Smith, W.G., Seibert, K., Isakson, P.C., 2002. Pharmacology of celecoxib in rat brain after kainate administration. J. Pharmacol. Exp. Ther. 302, 846–852.

Coghill, R.C., Sang, C.N., Maisog, J.M., Iadarola, M.J., 1999. Pain intensity processing within the human brain: a bilateral, distributed mechanism. J. Neurophysiol. 82, 1934–1943.

Cohen, M.X., Schoene-Bake, J.C., Elger, C.E., Weber, B., 2009. Connectivity-based segregation of the human striatum predicts personality characteristics. Nat. Neurosci. 12, 32–34.

Craig, A.D., Chen, K., Bandy, D., Reiman, E.M., 2000. Thermosensory activation of insular cortex. Nat. Neurosci. 3, 184–190.

Deyama, S., Nakagawa, T., Kaneko, S., Uehara, T., Minami, M., 2007. Involvement of the bed nucleus of the stria terminalis in the negative affective component of visceral and somatic pain in rats. Behav. Brain Res. 176, 367–371.

Fang, J., Shing, Y., Wiederschain, D., Yan, L., Butterfield, C., Jackson, G., Harper, J., Tamvakopoulos, G., Moses, M.A., 2000. Matrix metalloproteinase-2 is required for the switch to the angiogenic phenotype in a tumor model. Proc. Natl. Acad. Sci. U. S. A. 97, 3884–3889.

Ferland, C.E., Laverty, S., Beaudry, F., Vachon, P., 2011. Gait analysis and pain response of two rodent models of osteoarthritis. Pharmacol. Biochem. Behav. 97, 603–610.

Fosang, A.J., Neame, P.J., Last, K., Hardingham, T.E., Murphy, G., Hamilton, J.A., 1992. The interglobular domain of cartilage aggrecan is cleaved by PUMP, gelatinases, and cathepsin B. J. Biol. Chem. 267, 19470–19474.

Franca, D.S., Ferreira-Alves, D.L., Duarte, I.D., Ribeiro, M.C., Rezende, R.M., Bakhle, Y.S., Francischi, J.N., 2006. Endogenous opioids mediate the hypoalgesia induced by selective inhibitors of cyclo-oxygenase 2 in rat paws treated with carrageenan. Neuropharmacology 51, 37–43.

Gear, R.W., Aley, K.O., Levine, J.D., 1999. Pain-induced analgesia mediated by mesolimbic reward circuits. J. Neurosci. 19, 7175–7181.

Gijbels, K., Masure, S., Carton, H., Opdenakker, G., 1992. Gelatinase in the cerebrospinal fluid of patients with multiple sclerosis and other inflammatory neurological disorders. J. Neuroimmunol. 41, 29–34.

Governo, R.J.M., Morris, P.G., Marsden CA Chapman, V., 2008. Gabapentin evoked changes in functional activity in nociceptive regions in the brain of the anaesthetized rat: an fMRI study. Br. J. Pharmacol. 153, 1558–1567.

Gum, R.J., Hickman, D., Fagerland, J.A., Heindel, M.A., Gagne, G.D., Schmidt, J.M., Michaelides, M.R., Davidsen, S.K., Ulrich, R.G., 2001. Analysis of two matrix metalloproteinase inhibitors and their metabolites for induction of phospholipidosis in rat and human hepatocytes(1). Biochem. Pharmacol. 62, 1661–1673.

Gustin, S.M., Peck, C.C., Wilcox, S.L., Nash, P.G., Murray, G.M., Henderson, L.A., 2011. Different pain, different brain: thalamic anatomy in neuropathic and non-neuropathic chronic pain syndromes. J. Neurosci. 31, 5956–5964.

Gwilym, S.E., Filippini, N., Douaud, G., Carr, A.J., Tracey, I., 2010. Thalamic atrophy associated with painful osteoarthritis of the hip is reversible after arthroplasty: a longitudinal voxel-based morphometric study. Arthritis Rheum. 62, 2930–2940.

Harris, R.E., Clauw, D.J., Scott, D.J., McLean, S.A., Gracely, R.H., Zubieta, J.K., 2007. Decreased central mu-opioid receptor availability in fibromyalgia. J. Neurosci. 27, 10000–10006.

Heathfield, T.F., Onnerfjord, P., Dahlberg, L., Heinegard, D., 2004. Cleavage of fibromodulin in cartilage explants involves removal of the N-terminal tyrosine sulfate-rich region by proteolysis at a site that is sensitive to matrix metalloproteinase-13. J. Biol. Chem. 279, 6286–6295.

Heinegard, D., Saxne, T., 2011. The role of the cartilage matrix in osteoarthritis. Nat. Rev. Rheumatol. 7, 50–56.

Itoh, T., Matsuda, H., Tanioka, M., Kuwabara, K., Itohara, S., Suzuki, R., 2002. The role of matrix metalloproteinase-2 and matrix metalloproteinase-9 in antibody-induced arthritis. J. Immunol. 169, 2643–2647.

Jbabdi, S., Woolrich, M.W., Behrens, T.E., 2009. Multiple-subjects connectivity-based parcellation using hierarchical Dirichlet process mixture models. NeuroImage 44, 373–384.

Jenkins, B.G., 2012. Pharmacologic magnetic resonance imaging (phMRI): imaging drug action in the brain. NeuroImage 62, 1072–1085.

Ji, R.R., Xu, Z.Z., Wang, X., Lo, E.H., 2009. Matrix metalloprotease regulation of neuropathic pain. Trends Pharmacol. Sci. 30, 336–340.

Kawasaki, Y., Xu, Z.Z., Wang, X., Park, J.Y., Zhuang, Z.Y., Tan, P.H., Gao, Y.J., Roy, K., Corfas, G., Lo, E.H., Ji, R.R., 2008. Distinct roles of matrix metalloproteases in the early- and late-phase development of neuropathic pain. Nat. Med 14, 331–336.

Kenshalo Jr., D.R., Giesler Jr., G.J., Leonard, R.B., Willis, W.D., 1980. Responses of neurons in primate ventral posterior lateral nucleus to noxious stimuli. J. Neurophysiol. 43, 1594–1614.

Linnman, C., Moulton, E.A., Barmettler, G., Becerra, L., Borsook, D., 2011. Neuroimaging of the periaqueductal gray: state of the field. NeuroImage 60, 505–522.

Little, C.B., Barai, A., Burkhardt, D., Smith, S.M., Fosang, A.J., Werb, Z., Shah, M., Thompson, E.W., 2009. Matrix metalloproteinase 13-deficient mice are resistant to osteoarthritic cartilage erosion but not chondrocyte hypertrophy or osteophyte development. Arthritis Rheum. 60, 3723–3733.

Lorenz, J., Minoshima, S., Casey, K.L., 2003. Keeping pain out of mind: the role of the dorsolateral prefrontal cortex in pain modulation. Brain 126, 1079–1091.

Lu, H., Zou, Q., Gu, H., Raichle, M.E., Stein, E.A., Yang, Y., 2012. Rat brains also have a default mode network. Proc. Natl. Acad. Sci. U. S. A. 109, 3979–3984.

Michaluk, P., Wawrzyniak, M., Alot, P., Szczot, M., Wyrembek, P., Mercik, K., Medvedev, N., Wilczek, E., De Roo, M., Zuschratter, W., Muller, D., Wilczynski, G.M., Mozrzymas, J.W., Stewart, M.G., Kaczmarek, L., Wlodarczyk, J., 2011. Influence of matrix metalloproteinase MMP-9 on dendritic spine morphology. J. Cell Sci. 124, 3369–3380.

Mizoguchi, H., Yamada, K., Nabeshima, T., 2011. Matrix metalloproteinases contribute to neuronal dysfunction in animal models of drug dependence, Alzheimer's disease, and epilepsy. Biochem. Res. Int. 2011, 681385.

Morano, T.J., Bailey, N.J., Cahill, C.M., Dumont, E.C., 2008. Nuclei-and condition-specific responses to pain in the bed nucleus of the stria terminalis. Prog. Neuropsychopharmacol. Biol. Psychiatry 32, 643–650.

Napadow, V., LaCount, L., Park, K., As-Sanie, S., Clauw, D.J., Harris, R.E., 2010. Intrinsic brain connectivity in fibromyalgia is associated with chronic pain intensity. Arthritis Rheum. 62, 2545–2555.

Napadow, V., Kim, J., Clauw, D.J., Harris, R.E., 2012. Decreased intrinsic brain connectivity is associated with reduced clinical pain in fibromyalgia. Arthritis Rheum. 64, 2398–2403.

Nguyen, Q., Murphy, G., Hughes, C.E., Mort, J.S., Roughley, P.J., 1993. Matrix metalloproteinases cleave at two distinct sites on human cartilage link protein. Biochem. J. 295 (Pt 2), 595–598.

Okun, A., Liu, P., Davis, P., Ren, J., Remeniuk, B., Brion, T., Ossipov, M.H., Xie, J., Dussor, G.O., King, T., Porreca, F., 2012. Afferent drive elicits ongoing pain in a model of advanced osteoarthritis. Pain 153, 924–933.

Ostrowsky, K., Magnin, M., Ryvlin, P., Isnard, J., Guenot, M., Mauguiere, F., 2002. Representation of pain and somatic sensation in the human insula: a study of responses to direct electrical cortical stimulation. Cereb. Cortex 12, 376–385.

Paulson, S.K., Zhang, J.Y., Breau, A.P., Hribar, J.D., Liu, N.W., Jessen, S.M., Lawal, Y.M., Cogburn, J.N., Gresk, C.J., Markos, C.S., Maziasz, T.J., Schoenhard, G.L., Burton, E.G., 2000. Pharmacokinetics, tissue distribution, metabolism, and excretion of celecoxib in rats. Drug Metab. Dispos. 28, 514–521.

Paxinos, G., Watson, C., 2009. The rat brain in stereotaxic coordinates. Academic Press, San Diego, CA.

Pendse, G.V., Schwarz, A.J., Baumgartner, R., Coimbra, A., Upadhyay, J., Borsook, D., Becerra, L., 2010. Robust, unbiased general linear model estimation of phMRI signal amplitude in the presence of variation in the temporal response profile. J. Magn. Reson. Imaging 31, 1445–1457.

Porro, C., 2003. Functional imaging and pain: behavior, perception, and modulation. Neuroscientist 9, 354–369.

Rezende, R.M., Dos Reis, W.G., Duarte, I.D., Lima, P.P., Bakhle, Y.S., de Francischi, J.N., 2009. The analgesic actions of centrally administered celecoxib are mediated by endogenous opioids. Pain 142, 94–100.

Rodriguez-Raecke, R., Niemeier, A., Ihle, K., Ruether, W., May, A., 2009. Brain gray matter decrease in chronic pain is the consequence and not the cause of pain. J. Neurosci. 29, 13746–13750.
Romanic, A.M., White, R.F., Arleth, A.J., Ohlstein, E.H., Barone, F.C., 1998. Matrix metalloproteinase expression increases after cerebral focal ischemia in rats: inhibition of matrix metalloproteinase-9 reduces infarct size. Stroke 29, 1020–1030.
Rosenberg, G.A., Navratil, M., Barone, F., Feuerstein, G., 1996. Proteolytic cascade enzymes increase in focal cerebral ischemia in rat. J. Cereb. Blood Flow Metab. 16, 360–366.
Samad, T.A., Moore, K.A., Sapirstein, A., Billet, S., Allchorne, A., Poole, S., Bonventre, J.V., Woolf, C.J., 2001. Interleukin-1beta-mediated induction of Cox-2 in the CNS contributes to inflammatory pain hypersensitivity. Nature 410, 471–475.
Sanchez-Pernaute, R., Ferree, A., Cooper, O., Yu, M., Brownell, A.L., Isacson, O., 2004. Selective COX-2 inhibition prevents progressive dopamine neuron degeneration in a rat model of Parkinson's disease. J. Neuroinflammation 1, 6.
Seifert, F., Maihofner, C., 2011. Functional and structural imaging of pain-induced neuroplasticity. Curr. Opin. Anaesthesiol. 24, 515–523.
Sekine-Aizawa, Y., Hama, E., Watanabe, K., Tsubuki, S., Kanai-Azuma, M., Kanai, Y., Arai, H., Aizawa, H., Iwata, N., Saido, T.C., 2001. Matrix metalloproteinase (MMP) system in brain: identification and characterization of brain-specific MMP highly expressed in cerebellum. Eur. J. Neurosci. 13, 935–948.
Seminowicz, D.A., Laferriere, A.L., Millecamps, M., Yu, J.S., Coderre, T.J., Bushnell, M.C., 2009. MRI structural brain changes associated with sensory and emotional function in a rat model of long-term neuropathic pain. NeuroImage 47, 1007–1014.
Shih, Y.Y., Chen, C.C., Shyu, B.C., Lin, Z.J., Chiang, Y.C., Jaw, F.S., Chen, Y.Y., Chang, C., 2009. A new scenario for negative functional magnetic resonance imaging signals: endogenous neurotransmission. J. Neurosci. 29, 3036–3044.
Sotres-Bayon, F., Torres-Lopez, E., Lopez-Avila, A., del Angel, R., Pellicer, F., 2001. Lesion and electrical stimulation of the ventral tegmental area modify persistent nociceptive behavior in the rat. Brain Res. 898, 342–349.
Takemura, Y., Yamashita, A., Horiuchi, H., Furuya, M., Yanase, M., Niikura, K., Imai, S., Hatakeyama, N., Kinoshita, H., Tsukiyama, Y., Senba, E., Matoba, M., Kuzumaki, N., Yamazaki, M., Suzuki, T., Narita, M., 2011. Effects of gabapentin on brain hyperactivity related to pain and sleep disturbance under a neuropathic pain-like state using fMRI and brain wave analysis. Synapse 65, 668–676.
Tu, C.H., Niddam, D.M., Chao, H.T., Chen, L.F., Chen, Y.S., Wu, Y.T., Yeh, T.C., Lirng, J.F., Hsieh, J.C., 2010. Brain morphological changes associated with cyclic menstrual pain. Pain 150, 462–468.
Upadhyay, J., Maleki, N., Potter, J., Elman, I., Rudrauf, D., Knudsen, J., Wallin, D., Pendse, G., McDonald, L., Griffin, M., Anderson, J., Nutile, L., Renshaw, P., Weiss, R., Becerra, L., Borsook, D., 2010. Alterations in brain structure and functional connectivity in prescription opioid-dependent patients. Brain 133, 2098–2114.
Upadhyay, J., Anderson, J., Schwarz, A.J., Coimbra, A., Baumgartner, R., Pendse, G., George, E., Nutile, L., Wallin, D., Bishop, J., Neni, S., Maier, G., Iyengar, S., Evelhoch, J.L., Bleakman, D., Hargreaves, R., Becerra, L., Borsook, D., 2011a. Imaging drugs with and without clinical analgesic efficacy. Neuropsychopharmacology 36, 2659–2673.
Upadhyay, J., Baker, S.J., Chandran, P., Miller, L., Lee, Y., Marek, G.J., Sakoglu, U., Chin, C.L., Luo, F., Fox, G.B., Day, M., 2011b. Default-mode-like network activation in awake rodents. PLoS One 6, e27839.
Vanegas, H., Schaible, H.G., 2001. Prostaglandins and cyclooxygenases [correction of cycloxygenases] in the spinal cord. Prog. Neurobiol. 64, 327–363.
Voorn, P., Vanderschuren, L.J., Groenewegen, H.J., Robbins, T.W., Pennartz, C.M., 2004. Putting a spin on the dorsal-ventral divide of the striatum. Trends Neurosci. 27, 468–474.
Wada, C.K., Holms, J.H., Curtin, M.L., Dai, Y., Florjancic, A.S., Garland, R.B., Guo, Y., Heyman, H.R., Stacey, J.R., Steinman, D.H., Albert, D.H., Bouska, J.J., Elmore, I.N., Goodfellow, C.L., Marcotte, P.A., Tapang, P., Morgan, D.W., Michaelides, M.R., Davidsen, S.K., 2002. Phenoxyphenyl sulfone N-formylhydroxylamines (retrohydroxamates) as potent, selective, orally bioavailable matrix metalloproteinase inhibitors. J. Med. Chem. 45, 219–232.
Wang, Y.X., 2008. In vivo magnetic resonance imaging of animal models of knee osteoarthritis. Lab. Anim. 42, 246–264.
Wartolowska, K., Hough, M.G., Jenkinson, M., Andersson, J., Wordsworth, B.P., Tracey, I., 2012. Structural changes of the brain in rheumatoid arthritis. Arthritis Rheum. 64, 371–379.
Waubant, E., Goodkin, D.E., Gee, L., Bacchetti, P., Sloan, R., Stewart, T., Andersson, P.B., Stabler, G., Miller, K., 1999. Serum MMP-9 and TIMP-1 levels are related to MRI activity in relapsing multiple sclerosis. Neurology 53, 1397–1401.
Woolf, C.J., Salter, M.W., 2000. Neuronal plasticity: increasing the gain in pain. Science 288, 1765–1769.
Woolrich, M.W., Jbabdi, S., Patenaude, B., Chappell, M., Makni, S., Behrens, T., Beckmann, C., Jenkinson, M., Smith, S.M., 2009. Bayesian analysis of neuroimaging data in FSL. NeuroImage 45, S173–S186.
Xie, Z., Liachenko, S., Chiao, P.C., Carvajal-Gonzalez, S., Bove, S., Bocan, T., 2010. In vivo MRI assessment of knee cartilage in the medial meniscal tear model of osteoarthritis in rats. Med. Image Comput. Comput. Assist. Interv. 13, 57–64.
Yamagata, K., Andreasson, K.I., Kaufmann, W.E., Barnes, C.A., Worley, P.F., 1993. Expression of a mitogen-inducible cyclooxygenase in brain neurons: regulation by synaptic activity and glucocorticoids. Neuron 11, 371–386.
Yong, V.W., Power, C., Forsyth, P., Edwards, D.R., 2001. Metalloproteinases in biology and pathology of the nervous system. Nat. Rev. Neurosci. 2, 502–511.
Zhao, F., Welsh, D., Williams, M., Coimbra, A., Urban, M.O., Hargreaves, R., Evelhoch, J., Williams, D.S., 2012. fMRI of pain processing in the brain: a within-animal comparative study of BOLD vs. CBV and noxious electrical vs. noxious mechanical stimulation in rat. NeuroImage 59, 1168–1179.
Zubieta, J.K., Smith, Y.R., Bueller, J.A., Xu, Y., Kilbourn, M.R., Jewett, D.M., Meyer, C.R., Koeppe, R.A., Stohler, C.S., 2001. Regional mu opioid receptor regulation of sensory and affective dimensions of pain. Science 293, 311–315.